Fusion Engineering and Design 179 (2022) 113122

Contents lists available at ScienceDirect

Fusion Engineering and Design

journal homepage: www.elsevier.com/locate/fusengdes

Development of a concept and basis for the DEMO diagnostic and control system

W. Biel [a,b,*], M. Ariola [c], I. Bolshakova [d], K.J. Brunner [e], M. Cecconello [f], I. Duran [g], Th. Franke [h,i], L. Giacomelli [j], L. Giannone [h], F. Janky [h], A. Krimmer [a], R. Luis [k], A. Malaquias [k], G. Marchiori [l], O. Marchuk [a], D. Mazon [m], A. Pironti [n], A. Quercia [n], N. Rispoli [j], S. El Shawish [o], M. Siccinio [h,i], A. Silva [k], C. Sozzi [j], G. Tartaglione [c], T. Todd [p], W. Treutterer [h], H. Zohm [h]

[a] Institut für Energie- und Klimaforschung, Forschungszentrum Jülich GmbH, Germany
[b] Department of Applied Physics, Ghent University, Belgium
[c] Universita' di Napoli "Parthenope", Consorzio CREATE, Italy
[d] Magnetic sensor laboratory, Lviv, Ukraine
[e] Max-Planck-Institut für Plasmaphysik, Greifswald, Germany
[f] Department of Physics and Astronomy, Uppsala University, Sweden
[g] Institute of Plasma Physics, Czech Academy of Science, Praha, Czech Republic
[h] Max-Planck-Institut für Plasmaphysik, Garching, Germany
[i] EUROfusion Power Plant Physics and Technology (PPPT) department, Garching, Germany
[j] ISTP-CNR, Istituto per la Scienza e Tecnologia dei Plasmi, Milano, Italy
[k] Instituto de Plasmas e Fusão Nuclear, IST, Universidade de Lisboa, Portugal
[l] Consorzio RFX (CNR, ENEA, INFN, Università di Padova), Padova, Italy
[m] CEA, IRFM, F-13108 Saint Paul-lez-Durance, France
[n] Università degli Studi di Napoli Federico II, Consorzio CREATE, Italy
[o] Jožef Stefan Institute, Ljubljana, Slovenia
[p] UKAEA, Abingdon, UK (retired)

ARTICLE INFO

Keywords:
DEMO
Tokamak
Plasma diagnostics
Plasma control

ABSTRACT

An initial concept for the plasma diagnostic and control (D&C) system has been developed as part of European studies towards the development of a demonstration tokamak fusion reactor (DEMO). The main objective is to develop a feasible, integrated concept design of the DEMO D&C system that can provide reliable plasma control and high performance (electricity output) over extended periods of operation. While the fusion power is maximized when operating near to the operational limits of the tokamak, the reliability of operation typically improves when choosing parameters significantly distant from these limits. In addition to these conflicting requirements, the D&C development has to cope with strong adverse effects acting on all in vessel components on DEMO (harsh neutron environment, particle fluxes, temperatures, electromagnetic forces, etc.). Moreover, space allocation and plasma access are constrained by the needs for first wall integrity and optimization of tritium breeding. Taking into account these boundary conditions, the main DEMO plasma control issues have been formulated, and a list of diagnostic systems and channels needed for plasma control has been developed, which were selected for their robustness and the required coverage of control issues. For a validation and refinement of this concept, simulation tools are being refined and applied for equilibrium, kinetic and mode control studies.

1. Introduction and overview

The European long-term strategy towards fusion energy foresees the development of a demonstration fusion reactor (DEMO) as the single step between the tokamak experiment ITER and a commercial fusion power plant. According to the European roadmap for fusion [1], DEMO is expected to deliver significant net electrical power to the grid by the middle of the 21st century, achieve tritium self-sufficiency, and allow for

* Corresponding author at: Institute for Energy and Climate Research, Forschungszentrum Juelich GmbH, Leo-Brandt-Str, Juelich, Germany.
E-mail address: w.biel@fz-juelich.de (W. Biel).

https://doi.org/10.1016/j.fusengdes.2022.113122
Received 14 September 2021; Received in revised form 26 January 2022; Accepted 28 March 2022
Available online 7 April 2022
0920-3796/© 2022 The Authors. Published by Elsevier B.V. This is an open access article under the CC BY license (http://creativecommons.org/licenses/by/4.0/).

a credible extrapolation towards the economic viability of a commercial fusion power plant. The current pre-conceptual studies on the development of the European DEMO reactor follow a conservative approach [2–4] using only moderate physics and technology extrapolations beyond the status of ITER. This approach is chosen in order to facilitate a timely development of DEMO under the boundary conditions of limited resources, and it takes into account the delays of ITER construction, which are shifting the schedule for large-scale experimental validation of any major new developments on ITER towards the late 2030s or the 2040s.

The DEMO baseline design under consideration, for which an initial D&C concept has been developed here, is a tokamak with predominantly inductively driven long pulse operation (a few hours) and several 100 MWs of net electrical output power. Some details on the DEMO design concept and architecture are presented in [2,3,5–9]. Regarding the plasma scenario for this European DEMO tokamak reactor, it is currently assumed [10,11] that the plasma confinement properties will be near to the standard ELMy H-mode (confinement quality H ~ 1.0, see [12]), but without edge localized modes (ELMs) or with only low energy ELMs below the threshold for plasma facing component damage. Moreover, operation with high core plasma radiation fraction P_{rad}/P_{heat} ~ 0.6-0.7 is foreseen in order to limit the power flowing towards the divertor, and in particular with high plasma density to facilitate detached plasma operation in the proposed lower single-null divertor. The typical time-averaged auxiliary plasma heating power P_{aux} applied would be in the order of 50 MW or less, to be used mainly for the control of plasma operation but with only minor impact on the pulse duration via current drive. Further details on the current physics basis and their gaps have been published, see refs. [10] and [13]. A few technical parameters and expected performance data of DEMO are summarised in Table 1 [10].

It is important to note that not all of the key features of the DEMO plasma scenario and technology are well defined yet, nor have they been simultaneously demonstrated in large experiments under relevant conditions so far. Also, there are no detailed DEMO requirements and there is no DEMO operational plan available yet, from which specific requirements and arguments on design choices for the D&C development could be based on. However, the European strategy on DEMO [1,2] foresees a fast progress towards a feasible plant concept, requiring work in parallel on all open issues in DEMO physics and technology. Therefore, in this initial phase of the European DEMO studies, the development of the DEMO diagnostic and control (D&C) system is being pursued in a generic and flexible manner, taking up the above-mentioned assumptions but also considering the significant uncertainties concerning the definition of the final plasma scenario and machine properties, aiming to provide valuable contributions to resolving the open issues for the overall DEMO concept, in close collaboration with all other work packages. More details on the general DEMO design approach are given in [4,14]. Of course it cannot be excluded at this time that, with the overall progress on the understanding of DEMO physics and technology, some additional needs for specific developments also in the area of D&C may come up in future.

The first tokamak experiment producing significant fusion power will be ITER. Given the plasma parameters and the nuclear environment of the ITER machine, the ongoing developments for the ITER D&C system are an important knowledge basis for all considerations towards DEMO diagnostic and control. The ITER diagnostic suite under development [15,16] has to serve the needs for both plasma control and physics investigations in a plasma experiment with predominantly alpha particle heating and moderate neutron fluence up to damage levels in the order of one displacement per atom (1 dpa) near the first wall. The engineering challenges for the realization of ITER diagnostics [17–19] and in particular the nuclear aspects [20] have led to the development of important concepts such as the port plug based integration approach, the maintenance of diagnostic components via remote handling and the selection of irradiation-hard functional materials for diagnostics components. Many of these ITER diagnostic concepts can be taken over for DEMO, some however need proper adaptation to the specific DEMO conditions.

Table 1
Key parameters of the EU DEMO tokamak concept.

Parameter	Symbol	Value/Range
Major plasma radius	R_0	9 m
Minor plasma radius	a	2.9 m
Toroidal magnetic field on axis	B_0	5.8 T
Plasma current	I_p	17.7 MA
Plasma elongation	κ_{95}	1.65
Fusion power	P_{fus}	2 GW
Installed auxiliary heating power	P_{aux}	130-150 MW
Pulse duration	t_{pulse}	2 h
Net electrical output power	$P_{el,net}$	300-500 MW

In addition to the open questions about the DEMO physics basis and the definition and validation of the plasma scenario, the development of the DEMO plasma D&C system is facing a number of significant challenges [21–23], which go far beyond the requirements for ITER. These include on the one hand the high reliability demands on the control near operational limits, and on the other hand technical and space limitations for the integration of D&C subsystems into the machine with strong loads acting onto all components, leading to limited performance of the D&C system. In order to ensure tight regulation of the DEMO plasma in view of these challenges and limitations, estimation and control techniques will be employed, which aim to provide both a fast description of the plasma state based on the full set of measured data, and model-based based predictions towards optimized actuator control trajectories [24]. However, the possibility of adopting such techniques depends on the availability of accurate models, which need to be validated on currently operating tokamaks, and then extrapolated to DEMO.

As part of the European DEMO design studies, the development of the D&C system has been launched in 2015 within the work package “DEMO diagnostic and control” (WPDC) [22]. During the first years of the project, an initial understanding of the prime choices of diagnostic methods and actuators applicable to DEMO has been obtained, and an initial version of the main DEMO control requirements has been developed. In order to prepare the physics models for future advanced control schemes, and to provide some quantitative verification towards the controllability of the DEMO plasma, control simulations have been developed for a number of control issues. At present, the D&C concept mainly addresses the stationary burn phase of the discharge, including some of the transients which are expected to occur within it. The discharge ramp-up and ramp-down phases, the heating up towards the burn phase, as well as emergency actions such as disruption avoidance and mitigation will be investigated in more detail in the next phase of the project.

This paper is structured as follows: In chapter 2 the challenges and limitations towards integration of diagnostics for plasma control into DEMO are discussed, and some requirements and first conclusions relevant for the control system are formulated. In chapter 3, the initial DEMO D&C concept is presented, addressing only the stationary (burn) phase at the current stage of development. Chapter 4 gives an overview on the diagnostic systems foreseen and the key issues towards their implementation into DEMO, including port allocation. In chapter 5 the current status of the foreseen actuators and their performance properties are briefly summarized. Open and critical remaining issues are discussed in chapter 6, which is followed by a summary and conclusions.

2. Challenges for diagnostic integration on DEMO

The development of the DEMO D&C system and in particular the integration of diagnostics on DEMO for plasma control have to face significant challenges [21–23,25]:

First, the DEMO D&C system has to provide high reliability, since any loss of plasma control may result in loss of confinement or ultimately in

disruptions, where the latter may cause significant damage of the inner wall or other components of the machine. Second, high accuracy of the D&C system is needed in order to operate DEMO at an operational point near to limits given by physics and technology, at which the operation is typically prone to instability whereas the output power of the reactor is maximized. Third, fast and early reactions by the D&C system are required in particular in case of unforeseen events, such as e.g. component failure or a significant increase in radiative cooling following sudden impurity ingress into the core plasma. Especially for coping with such unexpected events, it is crucial to have precise measurements available for all quantities to be controlled in real time: the more demanding the control requirements, the more precise the measurements and control actions must be. Fourth, the measurement possibilities on DEMO are limited by space restrictions for the integration of diagnostic components, arising from the need to optimise the tritium breeding rate TBR in the blanket, and by strong adverse effects acting on the diagnostic front-end components (neutron and gamma radiation, heat loads, erosion and deposition) degrading the diagnostic components over time. Moreover, the nuclear environment of DEMO makes it necessary that any maintenance has to be performed by remote handling and is therefore technically challenging, expensive and time-consuming. Consequently all in-vessel components should be designed for a high degree of durability and reliability, such that the need for any interventions for scheduled and non-scheduled maintenance is minimized. Under such conditions, the use of several diagnostic methods currently adopted in operating tokamaks or ITER will be critical or even impossible on DEMO. Finally, the capabilities of the available actuators for plasma control (poloidal field coils, auxiliary heating and fuelling) impose their own limitations as well.

Reliably controlled plasma operation can only be achieved as long as accurate and timely information about the actual plasma state in the various regions (core, edge and divertor) is available. For normal plasma operation, a reduced set of measurements may be sufficient if control oriented plasma models are able to describe plasma evolutions with adequate accuracy. However, in view of the risk of unforeseen events, or combinations of them, such as the sudden failure of major components (e.g. coolant ingress into the plasma chamber or a quench in superconducting magnets), or the sudden increase of plasma radiation following impurity ingress into the core plasma (dust particles etc.), it remains an open question to what degree future control oriented models will be able to cover all possible evolutions of the plasma. Therefore, at the current stage of the DEMO D&C development, we have to assume that the information on the plasma state is based on a sufficiently detailed coverage by available measurements, together with the application of advanced control oriented models.

Based on the challenges discussed above, the following general design strategy for the DEMO D&C system can be formulated:

Plasma diagnostic methods for DEMO have to be chosen according to their robustness and reliability, and all in-vessel and in-port components of diagnostics and actuators have to be mounted in sufficiently set back (protected) locations and they should use robust designs and resilient materials, in order to maximize lifetime of the system components (to minimize maintenance needs and the resulting downtimes). The goal is to achieve maintenance-free operation of all in-vessel components over at least the designed blanket lifetime, i.e. two full power years (fpy) for the starter blanket which is designed for a neutron fluence consistent with 20 displacements per atom (dpa), and 5 fpy for the second blanket (50 dpa) [26]. On the other hand, since all these in-vessel components are required for DEMO operation, and failure cannot be completely excluded, their design has to be compatible with maintenance via remote handling, and a sufficient amount of redundancy in terms of number of channels and/or number of methods has to be included in the overall D&C concept. Related to the high nuclear loads, in-vessel diagnostic components should predominantly consist of metallic parts with active cooling, complemented by ceramic insulators in cases where necessary (e.g. magnetic sensors). For a number of ex-vessel components the requirements for maintenance-free operation can be somewhat reduced, provided that any necessary maintenance actions are technically possible within a short time and with low effort, such that the overall availability target of DEMO is not compromised. For any optical diagnostics, windows have to be placed at locations where the reduction of transmission by radiation induced absorption (RIA) remains low enough over the necessary long periods of operation, which might require using vacuum extensions beyond the port plugs. In particular some more sensitive parts such as radiation detectors, electronics or cameras should only be installed in ex-vessel positions such that occasional service or replacement could be performed without interrupting DEMO operation for longer periods. Finally, the goal of minimizing space requirements and cost requires that all reasonable efforts are made to limit the space occupation by all the in-vessel components and systems to be integrated into DEMO.

3. Initial version of the DEMO control concept

In the following section we present the current version of the principal approaches for the main plasma control issues and their allocation to diagnostics and actuators on DEMO, which are summarized in Table 2 and explained in some detail in the text below. As evident from the table, it is intended to cover all control issues with at least two different independent diagnostic methods. Based on this proposed allocation between control issues on diagnostics, no lack of measurements could be identified with respect to the main control issues for the burn phase of the DEMO discharges. In order to cope with a certain rate of failure of diagnostic channels during operation, it is foreseen to provide some additional level of redundancy for each control issue by using measurements from extra channels or lines of sight. For the port-based D&C systems (other than the bulky infrared (IR) polarimetry/interferometry), two independent instances of each system are proposed to be installed in different toroidal locations. The overall goal is to achieve a reliable knowledge of the plasma state over a wide range of parameters, and at the same time be able to distinguish between correct and faulty measurements by means of integrated data analysis.

The key elements and the general approach for the control strategy for the DEMO plasma are summarized in the following, including the current understanding on the diagnostics, actuators and control margins needed for reliable control. This selection and allocation of diagnostics and actuators has been mainly based on considering the stationary burn phase, however, according to the current understanding no additional systems are expected to be necessary for the transient phases, but some parameter ranges of individual subsystems might need to be extended.

The key elements address the conditions for controlling a discharge scenario similar to the standard H mode in a divertor tokamak (but without ELMs). In case of a different plasma scenario, some control issues may need to be modified or added. The control issues can be grouped into the three subtopics equilibrium control, kinetic control and the control of instabilities and unforeseen events.

3.1. Equilibrium control

Plasma position and shape depend on the interplay between magnetic forces and kinetic plasma pressure. More specifically, the horizontal plasma position mainly depends on the vertical field, plasma current and pressure, while the vertical plasma position in the elongated configuration, as defined by attractive forces acting from PF coils located above and below the plasma, is in principle unstable and needs to be constantly monitored and controlled on a time scale related to the growth rate of the vertical instability. Thus the prime actuators for position and shape control are the poloidal field coils, as well as the central solenoid (via the plasma current and via stray fields), but also the auxiliary heating (increase of heating power) and the plasma fuelling (affecting confinement properties) influence the plasma position and shape. Usually, in the design of the controller for plasma current,

Table 2
Control issues and related diagnostics suite and actuators on DEMO, updated version based on [22]. See also the control requirements from physics considerations given in sections 3.1, 3.2 and 3.3 below. PF = poloidal field; CS = central solenoid; FW = first wall; VDE = vertical displacement event; MW = microwave; ECE = electron cyclotron emission measurement; P_{rad} = radiated power from plasma; ECR = electron cyclotron resonance; IR = infrared; LH = low/high plasma confinement; DT = deuterium/tritium; MHD = magnetohydrodynamics; ECCD = electron cyclotron current drive.

Control issue	Operational limits	Main diagnostics	Main actuators and counter-measures
Equilibrium control			
Plasma current / edge safety factor q95	Safety factor limit (q95)	Magnetic diagnostics Faraday sensors	PF+CS coils Auxiliary heating
Plasma position and shape, incl. vertical and horizontal stability	Wall loads (FW and divertor) Max. Δz / VDE disruption	Magnetic diagnostics MW reflectometry, ECE Neutron/gamma diagnostics IR polarimetry/ interferometry Prad	PF+CS coils Auxiliary heating
Kinetic control / scenario control			
Plasma edge density (and temperature)	Density limit Stable confinement Access conditions for divertor detachment	Reflectometry (ECE) IR polarimetry/ interferometry Spectroscopy (pellet injection)	Pellet injection (fuel) Gas injection (ECR heating)
Fusion power	Wall loads (FW and div.) LH threshold	Neutron diagnostics Density and temp. measurements FW/ blanket and div. power (for calibration only)	Auxiliary heating Pellet injection (DT ratio) Impurity gas injection PF+CS coils (shaping)
Power flow across the separatrix	Radiation limit LH threshold, divertor loads	Spectroscopy+radiation meas. Plasma heating power (fusion power and auxiliary heating)	Gas injection (impurities + fuel) Pellet injection (fuel) Auxiliary heating
Divertor detachment and heat flux control	Divertor wall loads LH threshold	Spectroscopy+radiation meas.Thermography Divertor thermo-currents Core neutron flux + reflectometry	Gas injection (impurities + fuel) Pellet injection (fuel) PF coils
Control of instabilities and unforeseen events			
Plasma pressure (control need t.b.c.)	beta limit	Magnetic diagnostics Density and temp. measurements	Auxiliary heating Fuel + impurity injection
(MHD) plasma instabilities	various (→ disruptions)	Reflectometry, ECE Radiation power measurements Neutron/ gamma diagnostics IR polarimetry/ interferometry Magnetic diagnostics	Auxiliary heating ECCD PF coils
Unforeseen events (impurity ingress, component failure)	various (→ disruptions)	all	all
Disruption avoidance and prediction	various (→ disruptions)	all	Robust control algorithms to tolerate expected noise/disturbances; effective exception handling; effective predictors
Disruption mitigation	various	all	Matter injection to distribute wall loads and act against runaways

position and shape control, the auxiliary heating and the plasma fuelling are treated as "disturbances" and the performance of the controller is tested against some assigned behaviours of these disturbances.

The physics requirements for equilibrium control during flat-top operation have been formulated as follows:

3.1a) The plasma current I_p has to be controlled to within +/- 0.5 MA, such that the edge safety factor during flat-top operation always remains in the interval $q_{95} = 3.5$ +/- 0.1.

3.1b) The horizontal and vertical position of the current centroid have to be controlled such that an initial displacement of 15 cm from the nominal position can always be recovered, preserving a minimum distance between separatrix and first wall and limiters in all poloidal locations greater than 8 cm, in order to minimize the wall loads.

3.1c) The plasma shaping has to be controlled such that both the elongation κ and the triangularity δ remain within +/- 0.03 of their target values, respectively.

The rationale for the formulation of these requirements is briefly explained in the following.

The plasma current I_p, or the edge safety factor q_{95}, respectively, are among the defining parameters of the plasma scenario. As such, the first requirement has been chosen here as to sustain an operational mode similar to the ELMy H mode [12], allowing for reasonably stable operation (which improves by increasing q_{95} with respect to the ITER baseline, keeping away from the ultimate safety factor limit which is near to $q_{95} = 2$ [27]) while still providing good energy confinement (which would be maximised near the safety factor limit by virtue of the higher current). The second requirement addressing the plasma position has been formulated with the intention to keep the plasma away from the first walls (blanket), at a distance which is always sufficient avoid overloading the wall which could lead to damage via melting and/or impurity ingress followed by a disruption. Here we assume that any vertical or horizontal motion within the limits given in 3.1b) would be primarily a "rigid body" motion without major impact on the fusion power. The third requirement defines the control margins for the elongation and triangularity, where the actual size of the proposed margins (+/- 0.03) is believed to be achievable when taking into account the assumed measurement accuracy of both current centroid and separatrix position (few centimetres each) which serve as reference for the actual plasma shape control. It is of course intended to keep the variation of the plasma shape as small as reasonably achievable, since at constant plasma current the fusion power depends on the elongation somewhat stronger than linearly (e.g. for standard H mode, the confinement time scales as $\tau_E \sim \kappa^{0.78}$ [12] and an additional contribution comes via the variation of the plasma volume with elongation, $V_{plasma} \sim \kappa$). Moreover, for the pedestal pressure a scaling with triangularity as $p_{ped} \sim \delta^{0.83}$ has been found [28], which translates also into a somewhat stronger than linear dependence of the fusion power from δ. In summary, for all requirements on the equilibrium parameters, the proposed target parameters and their margins given above have been chosen according to the current understanding of the achievable measurement accuracies and the typical parameter variations occurring during control actions in the burn phase of DEMO discharges.

The primary diagnostics choice for the plasma current, position, and shape control on tokamaks is traditionally the in-vessel magnetic diagnostics, and also the control concept for ITER is following this approach, see e.g. [29] and references therein. Coil based measurements provide a signal proportional to the time derivative of the magnetic field, and hence the signals need to be integrated over time. However, during the long stationary burn phase, the raw signals to be integrated are essentially zero. This means that any spurious voltages originating from irradiation effects [20] could appear as slow "drifts" of the magnetic configuration, which would have to be corrected before using these signals as inputs for plasma control. Neutronics calculations for various DEMO blanket concepts under development [30] show that the predicted neutron fluence behind the DEMO blanket (at the mid-plane position on the inboard side) could reach values up to 10^{25} /m^2 per

full power year of operation, which corresponds to one displacement per atom (dpa).

A number of irradiation-induced effects which could disturb signals from magnetic sensors have been thoroughly investigated for ITER conditions. Specifically, a thermo-electric voltage can be generated via transmutation in the conductor, which is known as the radiation-induced thermoelectric sensitivity (RITES) [20]. Since this effect only slowly evolves with the accumulated fluence over the period of operation, it could to some extent be corrected based on the baseline signal level measured just prior to the start of a DEMO discharge. Another important effect is the parasitic voltage induced by thermal gradients inside the sensor (temperature-induced electromotive force, TIEMF) [20]. These could in principle be minimized by optimizing the sensor design and sensor cooling such that a fairly constant temperature distribution over the sensor is maintained during operation. For the low-temperature co-fired ceramics (LTCC) coil design developed for ITER, a temperature drop of < 1 K has been predicted based on simulations [31], which translates into a typical spurious voltage of 0.1 - 0.5 μV [32]. Finally, the signals transmitted via mineral insulated (MI) coaxial cables can be disturbed by the radiation-induced electromotive force (RIEMF) effect, which generates a current or voltage across the insulator via charged particles, created by gamma or neutron reactions [20]. Considering the large neutron fluence on DEMO and the long duration discharge over which all the spurious signal contributions will be integrated, it has to be expected that signals from in-vessel magnetic sensors on DEMO will be accordingly more influenced by irradiation-induced effects as compared to the ITER sensors. Several methods will be used to check and correct drifting signals from in-vessel inductive sensors. First, ex-vessel magnetic sensors will be used since they are shielded by the thick vacuum vessel and hence they experience irradiation effects which are about three orders of magnitude lower than for the in-vessel sensors located behind the blanket [30]. However, the eddy current shielding by the vacuum vessel will slow down the signals measured by ex-vessel magnetic sensors, such that the different frequency response has to be taken into account in the comparison with the in-vessel signals. As a second and complementary approach, the installation of Hall sensors is foreseen. These sensors provide raw signals proportional to the magnetic field rather than its time derivative, however with only small signal amplitudes (in the more radiation-hard versions) which are also temperature dependent. The measurement of the poloidal magnetic field could also be accomplished with Faraday optical detectors, which measure the rotation of the polarization of a laser beam within a transparent medium of high Verdet constant [21]. Since all types of glass are very sensitive against radiation induced absorption (RIA), the applicability of this detector type for in-vessel measurements still needs to be demonstrated. RIA would not occur in liquid 'fibres', but their applicability for reliable operation in a nuclear tokamak will need further investigations.

The current approach for the planning towards plasma position and shape control on DEMO pursues a risk mitigation strategy: Fast in-vessel measurements from magnetic coil based sensors are foreseen, but complemented by microwave reflectometry measurements. Indeed, to alleviate the problems related to drifting integrators or irradiation-induced effects in the magnetic pickup coils, reflectometry was proposed to backup or complement the standard magnetic based control in ITER [33], and a first attempt to perform a radial position control using reflectometry measurements has been demonstrated on the ASDEX Upgrade tokamak [34]. In-vessel Hall sensors will be added if their durability against DEMO relevant irradiation levels can be shown. In addition, ex-vessel magnetic measurements (both coil based and Hall sensor based) will be available to monitor slow changes of the magnetic configuration, and to provide a basis for correcting the apparent drifting of in-vessel magnetics coil signals as arising from their irradiation damage. Moreover, IR interferometry/polarimetry could provide signals for plasma position control during the ramp-up and ramp-down phase of the discharge, when the plasma cross section is not fully developed and hence the plasma edge is too far away from the reflectometry antennae in order to obtain useful data. Neutron/gamma diagnostics can contribute in the nuclear burn phase to define the position of the plasma centre (~current centroid), which will provide a useful corroboration of the information from reflectometry monitoring the position of the plasma boundary. Finally, the observation of protection limiters via spectroscopy and thermography could provide valuable signals in case the plasma would come too close to one of these limiters. Since any of the listed measurements would report a change of plasma position only with some uncertainty and with some delay, the requirement 3.1.b) formulated above was chosen to provide a sufficient margin to avoid any loss of the discharge due to the lack of controllability of the equilibrium. Also, the required value of 8 cm minimum distance of the separatrix from the wall represents a safe value avoiding too strong plasma-wall interactions and thus minimizing the additional impurity ingress during such plasma movements (the typical e-folding length of the plasma edge parameters amounts to a few centimetres, depending on plasma conditions).

It remains an important area of future research and development (R&D) to better determine the limits of the durability (lifetime) of in-vessel magnetics by irradiation testing and modelling, to find out how far the spurious voltages arising from these effects can be corrected for, or whether a sudden end of the usability of these sensors has to be expected, e.g. by swelling, cracking or disconnection of cables, and to optimize the designs and locations of sensors accordingly.

According to typical controller architectures adopted for plasma position, current and shape control [35,36] the envisaged controller for DEMO has the following structure:

- Vertical stabilization controller
- Plasma current controller
- Plasma shape and position controller, which in turn is divided in two components
- Current decoupling controller
- Shape controller

Different to other tokamaks, where there are coils dedicated to the vertical stabilization of the plasma configuration, in the current DEMO baseline design it is not possible to have a structural decoupling between the plasma shape and position controller, and the vertical stabilization controller. Hence this decoupling should be obtained by means of the controller algorithm using a suitable geometrical decomposition.

The current decoupling controller acts on an intermediate timescale; its task is to evaluate the voltages to be applied to the PF coils in order to track the reference PF coil currents coming from the shape controller to compensate for unforeseen disturbance. The shape controller acts on a slower timescale with respect to the current decoupling controller.

The vertical stabilization controller acts on a faster time scale and uses as actuator a suitable combination of PF voltages; this controller calculates the continually changing PF coil currents required to maintain the vertically unstable plasma in a dynamic equilibrium.

Finally, the plasma current controller is designed as a separate loop, with the aim of minimizing the coupling effects with the shape controller. The plasma current (inversely related to the edge safety factor q_{95}) will be controlled based on signals from magnetic sensors (in-vessel and ex-vessel inductive sensors and Hall sensors) measuring the related poloidal fields, and for the case of a pulsed DEMO tokamak the actuators are the central solenoid current as well as the (limited) auxiliary plasma current drive. The edge safety factor has to be kept precisely in the desired range (see physics requirement 3.1a above), with a relatively small control margin, since it belongs to the characterizing quantities for the plasma scenario, and it is relevant for certain MHD instabilities [37]. Additional ex-vessel magnetic measurements are foreseen for the diamagnetic energy and the loop voltage, respectively. Diamagnetic loops are needed to evaluate in real time the poloidal beta and hence the plasma energy [38], which are important input data for

the burn control. On the other hand, the loop voltage measurement contains mixed information regarding non-inductive current drive, plasma resistance and plasma inductance change; hence this measurement is useful for equilibrium control. In DEMO ex-vessel magnetic measurements will be used as backup of the correspondent in-vessel sensors.

The performance in controlling the horizontal plasma position in DEMO as measured by inductive magnetic diagnostics during an unexpected "loss of power" event (transition from H mode to L mode) by means of ex-vessel PF coils has been simulated using the CREATE-L model [39], see Figs. 1 and 2 [36].

The result of this simulation shows that the maximum horizontal movement of the plasma towards the inner wall (see gaps no. 1-4) reaches more than 20 cm, even with investing up to 700 MW of mostly reactive electrical power for the necessary change of the poloidal magnetic field via the external PF coils. This means that during this control action the minimum distance between plasma and inner wall becomes too small, violating the requirement 3.1b formulated above: indeed gap no. 1 (the inner radial gap) gets as close as 4 cm to the first wall.

The large power demand during this control action is resulting from the need to restore the horizontal force balance in the tokamak after the drop of the plasma pressure in this assumed HL transition, according to the well-known equation by Shafranov [40]. Fulfilling this power demand would require to implement expensive choices in the reactor design, including the dimensioning of power supplies and the addition of a sizeable energy storage to decouple the varying control power needs from the electrical grid. Therefore, more recently a preliminary study has been carried out to assess which improvement of performance can be obtained using in-vessel radial field control coils. As a result it has been

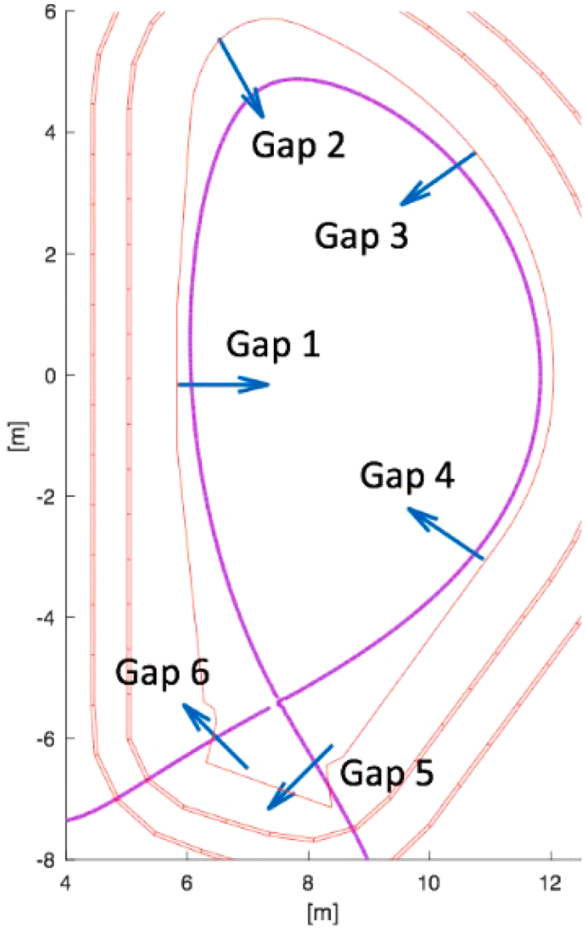

Fig. 1. Definition of the gaps between plasma edge and wall to be controlled.

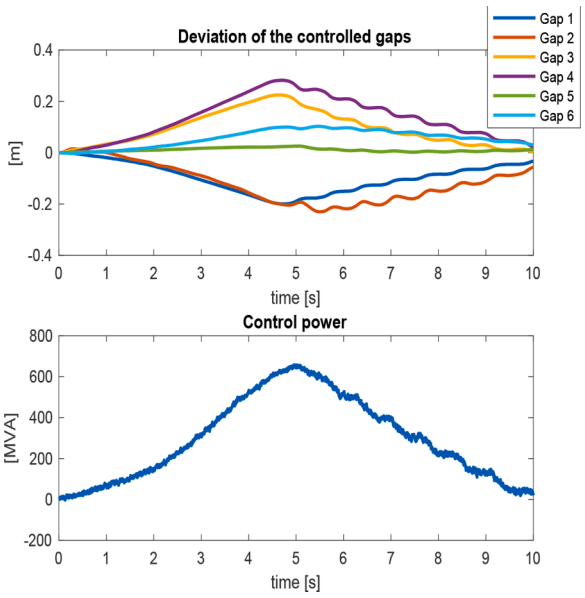

Fig. 2. Simulation results for the deviation of gaps and the required power to PF coils during the control action.

demonstrated that using these coils, whose positions have not been optimized yet, it is possible to control larger displacements than those recoverable just using ex-vessel control coils, with a much more limited control effort, in terms of required active and reactive power. Subsequent studies have shown that significant improvements are obtained resorting to in-vessel radial field control coils in counteracting a range of typical events that can occur during a DEMO discharge, both in terms of movements of the plasma boundary, and in terms of required control power. In comparison to ex vessel PF coils, in vessel control coils promise a faster control action onto the plasma at lower energy consumption, due to their lower inductivity and to the lower degree of eddy current shielding. However, a feasible design for in-vessel control coils with sufficient lifetime in DEMO has yet to be developed.

A preliminary evaluation of the performance in the reconstruction of the flux/field map at breakdown starting from the magnetic measurements has also been carried out, showing that the proposed set of sensors can be used for the scope, despite the presence of high eddy currents in the passive structure. However, the proposed reconstruction procedure is heavily based on the model which links the currents in the PF coils to the measurements. More studies have to be carried out in the future to propose a more robust reconstruction algorithm and to evaluate other effects such as 3D eddy currents affecting the measurements.

3.2. Kinetic control

Kinetic control comprises the control of kinetic plasma parameters in accordance with operational limits in the plasma, target fusion power P_{fus}, tolerable heat loads and low material erosion. Different approaches for the control of fusion power in a burning plasma like on ITER have already been investigated in great detail in earlier papers. More specifically, the control of fusion power by means of auxiliary power and fuelling rate (pellet injection and gas puffing) was studied based on a nonlinear 0D model for the plasma parameters, assuming equal temperatures for all particle species and considering plasma cooling by bremsstrahlung only [41]. Here it was found that a certain amount of auxiliary power is needed to counteract the instability ("thermal runaway") introduced by the nonlinear dependency of the fusion rate with the plasma temperature (here typically $T = 6$-8 keV were assumed as the operational point). A more recent study included the variation of the DT ratio as actuator, and used a refined radiation model including line radiation and recombination in addition to bremsstrahlung [42].

Finally, a more extended model was developed, where different temperatures for the electron and ion species were considered and the different heating mechanisms for electron and ion heating by the three auxiliary heating systems foreseen for ITER were included in the model [43]. All these studies have in common that, under the assumptions used here, a significant delay is observed between the action of auxiliary heating and the plasma response, as determined by the ratio between stored plasma energy and applied heating power. For the studies using the fuelling as actuator, the relatively long particle confinement time (τ_P > 10 s on ITER) represents the time scale on which the fusion power would react to any changes of fuelling rate or DT ratio. Turning now to burn control on DEMO, we have to take into account a few changes with respect to the case of ITER. First, for EU DEMO the main goal is to provide stable and high electricity output into the grid. Reacting on any reduction of fusion power by simply injecting additional auxiliary power can of course increase P_{fus} again, but in turn this control action could potentially reduce the net electrical output power of the reactor, as simulations with a systems code easily show when assuming realistic numbers for power conversion efficiencies and taking into account the possible power degradation in the energy confinement time (e.g. $\sim P^{-0.69}$ in eq. 30 of ref. [12]). In EU-DEMO, the burn control via (auxiliary) heating and current drive (H&CD) is also hampered by the high temperature (~35-40 keV) in the plasma centre, where most of the fusion reactions take place. At these temperatures in fact the equipartition time becomes very long (τ_{ei} > 30 s in the centre) and in addition all H&CD technologies primarily heat the electrons at these plasma parameters. Thus, the delayed heat transfer to the ions makes H&CD a rather slow actuator for P_{fus}. On the other hand, the high plasma temperature already lowers the increase of P_{fus} after any further temperature increase (central temperature near to the maximum of the fusion rate). Moreover, synchrotron radiation from the core plasma further damps the thermal runaway due to the large dependency from electron temperature ($P_{sync} \sim T^{2.6}$) [44]. Finally, in view of the extreme heat loads at the divertor target, all control actions affecting the fusion power will have to be carefully tailored with regard to the impact on the divertor plasma, in order to not exceed the heat load limits. In summary, for kinetic control on DEMO we will have to develop a refined approach, aiming to minimise the use of auxiliary power and considering all other possible actuator options potentially effecting the fusion power, including scenario control actions such as control of DT ratio, pedestal and core plasma density or plasma shaping (elongation κ and triangularity δ).

For a standard H mode discharge under DEMO conditions, a moderately peaked radial plasma density profile with a pedestal near the plasma edge is predicted [45,46]. The plasma density at the separatrix and at the pedestal top have a crucial importance for stable and reliable plasma operation in core and divertor region [47]. Specifically, divertor detachment can only be achieved and maintained under conditions of sufficiently large pedestal density [48]. On the other hand, understanding the Greenwald density limit [49] as a limit applying to the plasma edge density [50], the pedestal top density should remain below the Greenwald limit. This is in line with the experimental finding that when approaching the Greenwald limit, the power needed to sustain the H-mode increases much stronger than the linear scaling presented by Martin et al. [51]. Therefore, the actual size of the required margin will not only depend on the achievable accuracy for measuring and controlling the pedestal. Instead of the pedestal top density, alternatively the control of the separatrix density (at $r = a$) can be used [52] with regard to the density limit, avoiding a deterioration of the plasma confinement below H-mode levels.

The plasma pressure predicted for DEMO (based on confinement properties near to standard H mode) is currently predicted to stay significantly below the beta limit, such that developing a rigorous beta control as such is currently not amongst the priorities. Stable fusion power however requires maintaining the confinement quality, which requires controlling the power losses P_{sep} flowing across the separatrix. Finally, the power flowing into the divertor has to be limited or distributed over large areas such that the power load limitations of the divertor target plates are not exceeded. Another important aspect of divertor control is the limitation of erosion of the divertor target, which can be achieved by reducing the energy of impinging particles below the energy threshold for physical sputtering. The present understanding is that these conditions will be met when the divertor plasma shows a sufficiently high degree of detachment (low plasma temperature near the strike point, $T < 2$ eV).

The physics requirements for the kinetic control during the flat-top phase of the discharge have recently been formulated as follows:

3.2a) The electron density at the pedestal top should be controlled at a level of 85% of the Greenwald density limit, with a margin of +/- 5% of the Greenwald density.

3.2b) The fusion power should be controlled to keep the variations of fusion power always below +/- 20 percent over not more than 20 seconds.

3.2c) The power loss P_{sep} across the separatrix should be controlled to maintain a value of 1.2 times the confinement mode threshold (e.g. P_{LH}), where deviations of up to additional 50 MW within up to 20 seconds represent the tolerable limit.

3.2d) The divertor plasma will be controlled to maintain strongly detached plasma conditions, i.e. a high density plasma with a low temperature in front of the target of less than about 2 eV. It is assumed that under these conditions both the heat flux density and the erosion rate at the divertor targets are tolerable. Any loss of detachment ($T > 3$ eV) has to be recognized by the control system within less than 0.2 seconds, in order to allow turning on the strike point sweeping as a short-term measure against divertor overloading.

3.2e) The plasma pressure will be controlled such that the normalized plasma beta β_N will not exceed a value of 90% of the ideal beta limit.

The first requirement assumes that the Greenwald density limit [49] has to be understood as a limitation for the plasma pedestal top density. The proposed value and margin are taking into account the assumed accuracy of the measurement using microwave reflectometry, and the control actions via pellet injection leading to edge density variations of finite size. The second and third requirement were formulated based on the results of numerical simulations on burn control [53], which showed that the plasma can show strong reactions in P_{fus} and P_{sep} even after small disturbances and related control actions. Variations of the fusion power up to the limits formulated in requirement 3.2b) are not causing problems for electricity production, since the large thermal capacity of the blanket and coolant system results in a significant inertia (long time constant) which reduces the variation of coolant outlet temperature down to a tolerable level. The fourth requirement on divertor protection is based on the understanding that a direct measurement and control of the peak power flux in the divertor is not possible under DEMO conditions. Therefore, the existence of a relatively cold plasma region in front of the divertor (detachment) is postulated as a proxy, assuming that under detached conditions the heat flux density is in a tolerable range. After any loss of detachment, the control system should be able to react fast enough and with high priority (here: strike point sweeping [54], aiming to distribute the additional heat load over a larger area), where the short time constant given in 3.2d) is defined according to the time after which an overload would otherwise lead to severe divertor damage [55]. The current understanding is that the strike point sweeping can only be applied for limited periods in order to minimise divertor erosion. After turning on the sweeping either a controlled divertor detachment is soon achieved again, or the plasma has to be ramped down.

For the measurement of the plasma density, reflectometry is foreseen as the primary diagnostic in the gradient region, while the core electron density will be derived using infrared interferometry/polarimetry. The radial profiles from radiation power and neutron flux measurements may contribute to perform a consistency check of the density profiles. Primary actuators for density control are pellet and gas injection, while it is understood that the overall pumping speed and efficiency can only

slowly be adjusted deliberately, but may vary somewhat according to the actual divertor plasma conditions. For DEMO conditions, only pellets will have the deposition profile required to efficiently control the core density [56], while gas puffing may be used to control the separatrix/SOL/divertor density (and with it the neutral density in front of the pump). The accuracy of the density measurement for the pedestal top and separatrix density should be better than one third of the density control requirement as defined from physics (see the requirement 3.2a above). In order to investigate the possibilities and limitations of density measurements by reflectometry under DEMO plasma conditions, the full wave code REFMUL is being developed [57]. For the conditions applicable here, first simulations indicate that in absence of plasma turbulence a positional measurement accuracy of about 6 mm can be achieved with reflectometry in all poloidal positions where the curvature of the separatrix is low, corresponding to a measurement accuracy of 0.1e19 m^{-3} for the plasma density.

For a stable plasma operation in H mode or another high confinement regime, the power loss P_{sep} across the separatrix towards the divertor should exceed a certain power threshold, e.g. P_{LH} according to Martin et al. [51]. On the other hand, divertor protection requires keeping the local power fluxes on the divertor target below the damage threshold, which points towards reducing the loss power across the separatrix P_{sep} as much as possible. These two conflicting requirements on the loss power can only be fulfilled simultaneously by providing an accurate measurement of the plasma heating power (ionic part of fusion power $P_{fus,ion}$, and auxiliary power P_{ext}) together with the core plasma radiation power $P_{rad,core}$, and controlling their difference according to the relation

$$P_{sep} = P_{fus,ion} + P_{ext} - P_{rad,core} - \frac{\partial W}{\partial t} = f_{LH} P_{LH} \quad (1)$$

where the enhancement factor f_{LH} should be kept somewhat above unity ($f_{LH} \sim 1.2$) for stable H mode operation. In order to fulfil this condition for a DEMO tokamak with about 2 GW thermal power and an LH power threshold in the order of 100…150 MW (with a significant uncertainty at present which ideally will be reduced as the threshold scaling becomes more robust), the core radiation power typically has to amount 60…70% of the total plasma heating power. This makes the quantity P_{sep} a small difference of big numbers, with significant uncertainty as arising from the limited measurement accuracies for P_{heat}, $P_{rad,core}$ and the time derivative of the plasma energy W.

The main plasma diagnostics providing the signals for the control of P_{fus} and P_{sep} are the neutron flux and the total radiation power measurements, respectively. In order to achieve reliable signals for the control purposes, the neutron flux can be calibrated against data from activation foils (via accurate neutron transport models and simulations) and it can be in-situ cross-calibrated over long timescales against the measured thermal power transferred by the blanket and divertor cooling systems and the real-time activation of the first wall and/or divertor coolant, e.g. ^{16}N if the coolant contains oxygen. For the total plasma radiation power P_{rad} on DEMO, a stable absolute calibration of the measured signals cannot be guaranteed over long time. However, a relative calibration with respect to the H mode power threshold can be obtained by monitoring the radiation power signals during an LH- or HL-transition in the discharge, which is detectable e.g. via the temporal evolution of the radial density profile using reflectometry. A consistency check of these P_{rad} signals and a possible correction according to different impurity mixtures in the plasma can be achieved by providing additional measurements, e.g. a detailed spectroscopic analysis, together with on-line impurity transport and radiation modelling of the various contributions to core plasma radiation, where the measured plasma density and temperature profiles should be used as input. The achievable accuracy for these measurements and their calibrations, as well as the overshooting responses by the plasma to control actions, will inevitably result in some variation of P_{sep} during controlled operation.

The physics requirements for kinetic control points 3.2b) and 3.2c) above have therefore been formulated such that well defined deviations below the damage threshold of the machine are permitted for a limited period. Whether the formulations of the first four kinetic requirements would result in wall loads that are compatible with the heat load capability of the first wall and divertor under all possible conditions, still needs to be elaborated.

On the actuator side, the power balance and core radiation level can be adjusted by using impurity injection into the plasma core, fuel injection and auxiliary heating, where the latter is in particular applicable if a fast increase of heating power or a fast reduction of the radiated power fraction is needed (e.g. to counteract against an unwanted increase of plasma radiation and the subsequent reduction of P_{sep} arising from an impurity event). It should be noted here that the time response of impurity gas injection may be rather slow due to the long length of gas tubes between the valve and the injection point. As an alternative, pellet injection or laser ablation techniques would provide faster response, but at the expense of significant uncertainty of the amount of injected impurities. In both cases, the achievement of a viable working feedback control of impurity radiation for both core plasma and divertor plasma may be challenging.

According to the current understanding of plasma confinement, the predicted plasma pressure on DEMO will remain safely below the beta limit. In this sense, control of plasma pressure against the beta limit would already be assured by controlling fusion power within certain limits. On the time scale of the particle confinement time (in the order of $\tau_p \sim 30$ s for DEMO conditions [58]), the fusion power can be adjusted by replacing DT pellet injection into the core plasma by a number of D_2 pellets (change of DT ratio) or by helium gas injection (dilution of the DT fuel), by impurity pellet injection (temperature decrease via radiation cooling) or by reducing the plasma density and hence the fuel ion density. The reduction of the plasma shaping (elongation, triangularity), already mentioned in section 3.1 above, would provide a somewhat faster approach to reduce P_{fus}. All these options will be further analysed by simulations using a “flight simulator” kinetic code coupled to an equilibrium control code [11]. All these options will also be further assessed with regard to their compatibility to the tritium reprocessing [59] and to the stable operation of the chosen plasma scenario in terms of the acceptable range for P_{sep} and for the divertor loads.

The maximum target value for the plasma beta (requirement 3.2e) given above) has been defined to account for the current understanding of the required control margins. For the purpose of this plasma pressure limitation, a measurement of the diamagnetic energy will be performed via diamagnetic loops. This magnetic measurement will be amended by deriving a coarse electron temperature profile from ECE measurements (limited to the radial region where the electron density is high enough), and by deriving an ion temperature profile from gamma and neutron spectra, also taking into account high resolution X-ray spectra from the plasma centre. The plasma density profile follows from reflectometry and IR interferometry/polarimetry. The knowledge of plasma density and temperature profiles will not only improve the knowledge of the plasma energy (via integrated data analysis), but also allow performing a consistency-check of the fusion power and radiation power profiles in the plasma and thus enhance the robustness of the control concept.

If the plasma scenario would require a certain toroidal plasma rotation, an additional physics requirement would need to be added. Plasma rotation could be measured via the Doppler shift of high resolution X-ray spectra under the condition that the observation direction would have a horizontal inclination angle of, say, more than 10-15 degrees against the poloidal plane. Installing inclined lines of sight for X-ray spectroscopy would however increase the complexity and space occupation for this measurement as compared to the currently planned radial view installation. An alternative option could be collective Thomson scattering, which could potentially provide information on the ion velocity distribution and hence on the ion temperature and plasma rotation [60]. From the actuator side, neutral beam injection (NBI)

heating at an appropriate injection angle could be used to apply some torque to the plasma, where the feasibility of this approach under DEMO conditions is subject to further investigations. However, recently a decision was made to assume only electron cyclotron resonance heating (ECRH) as the baseline heating method during the next few years of development of EU DEMO, in order to focus resources on the heating system which is deemed as the closest to implementation, while still being capable of fulfilling the physics needs [61].

Within the divertor, the heat flux to each of the target plates has to be kept below the damage threshold. The current baseline foresees a strongly "detached" plasma state in front of the divertor, where the plasma temperature near the strike point is smaller than about 2 eV, and the particle density is accordingly high, such that only a partially ionized or even predominantly neutral particle zone exists in front of the target plates, which distributes the impinging heat loads onto a larger area and minimizes the target erosion [62].

The proposed approach for measurements for divertor detachment control is threefold: First of all, a spectroscopic analysis of the divertor plasma in front of the target plates is foreseen to identify the existence of a cold plasma zone (electron temperature $T_e < 2$ eV) and/or to determine the location of the ionization front of the detached plasma. The details regarding the decisive spectroscopic signature (selection of spectral lines or line shapes to be monitored; geometry of lines of sight) still need to be quantitatively verified, once a detailed control-oriented model of the divertor plasma becomes available. A preliminary analysis however indicates that the monitoring of high Balmer transitions of neutral hydrogen isotopes near the strike point could provide a promising signature of strong detachment (high density recombining plasma) via high line intensities together with Stark broadening, as was shown on Alcator [63] and JET [64]. An alternative promising spectroscopic signature of detachment has been demonstrated on TCV, where the Multispectral Advanced Narrowband Tokamak Imaging System (MANTIS) was used to detect a significant change in the geometric radiation pattern ("detachment front") in the divertor between attached and detached phases [65,66]. Secondly, the divertor thermo-currents shall be measured, which are related to the sheath voltage at the target plate and hence should drop almost to zero under conditions of low electron temperature near the target plates [67]. As a third approach, infrared thermography [68] will be employed to measure the local temperature distribution along the target plate. This third approach has the disadvantage that the "signal" is only received when the heating of the wall has already happened, i.e. the remaining time for corrective control actions is reduced accordingly. The spectroscopic and IR measurements will be implemented via first mirrors installed in the equatorial ports, such that the installation of optical components in the "dusty" divertor environment is avoided. Since the operational ranges of core plasma and divertor plasma are strongly linked, also the measured neutron flux can contribute to divertor control: an increase of neutron flux would indicate an increase of fusion power, which with some delay (slowing-down time of fusion alpha particles) would translate into a change of plasma heating power, and finally, with another delay given by energy confinement time, would lead to an increase of P_{sep} and power flow towards the divertor. Thus, a measured increase of neutron flux can already be used as input for control actions for the divertor plasma, to be undertaken earlier than the actual detachment measurements would allow.

The prime actuators for divertor plasma control are impurity and fuel injection into the edge and divertor plasma, and the control of the upstream (separatrix) plasma conditions, measured by reflectometry. The interrelation between the H mode control and the divertor power control, with partially contradicting requirements, the non-linear and indirect approaches for measurements, long time constants and/or inaccurate actuator response (impurity injection) and the rapid development of wall damage (erosion and melting) in case of failure, make this aspect of DEMO plasma control one of the most challenging ones.

In order to validate the applicability of the proposed kinetic control approach, a DEMO 'flight simulator' has been realized using the Automated System for TRansport Analysis (ASTRA) code [69] as plasma and a Simulink control environment to study control strategies, also taking into account simplified but realistic models of the physics (e.g. [48]) as well as the sensors and actuators as they emerge in WPDC and other EUROfusion work packages [53]. Different control schemes will be assessed by comparing their relative performance. This will also include the application of estimation methods to derive the plasma state from a different set of measurements, as well as advanced control methods where the plasma evolution is predicted in real time to improve the characterization of the plasma 'state' during the discharge [70,71]. In an iterative process, these studies will set the requirements for diagnostics and actuators, but will also point out in which parameter space the DEMO operational point can be controlled using realistic assumptions about the sensor and actuator performance.

Using this simulation code [53,72], the interplay between core and divertor radiation control has been simulated for two different assumed cases of argon compression ("enrichment") between core and divertor plasma, see Fig. 3 [73]. While for stronger enrichment (lower argon concentration in core plasma) the prescribed reattachment of the plasma can be controlled by adding argon into the divertor, the same approach fails in case of lower enrichment, since here the leaking of argon into the core plasma causes an HL transition, followed by a loss of control.

3.3. Remedies for instabilities and unforeseen events

Instabilities and unforeseen events are of major concern for the operation of DEMO, since they may ultimately lead to disruptions, which in turn have a significant potential to damage the machine.

The physics requirements for instability and event handling are not yet very detailed at this stage. They will be amended once further information becomes available. For the moment we can already define the following points:

3.3a) In case of island formation in the plasma, an island width of $w = 6$ cm should be clearly detectable by the control system within less than 0.1 seconds.

3.3b) The control system should be able to recognize any unplanned increase of plasma radiation greater than $dP_{rad}/dt > 0.1\ W_{kin}/\tau_E^2$ ("impurity events") within less than 0.2 seconds.

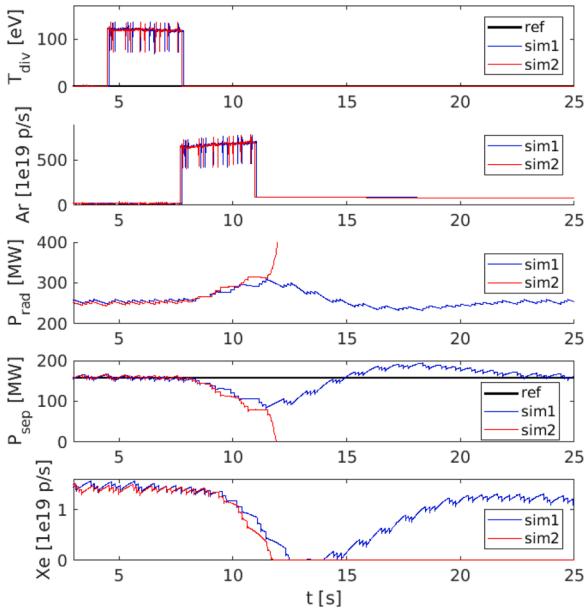

Fig. 3. Simulation of divertor detachment control after prescribed reattachment: sim1 with assumed argon enrichment factor 20; sim2 with enrichment factor 15 [73].

3.3c) The DEMO plasma should be ELM-free, or the ELMs should be smaller than 1 percent of the "natural ELMs" such that the deposited energy density onto the target plate remains below 0.1 MJ/m^2 per ELM.

Here, P_{rad} denotes the power radiated from the plasma, W_{kin} the kinetic energy content and τ_E the energy confinement time of the plasma. The numbers given in the first requirement follow from the results of performance studies (simulations) on the expected measurement performance of ECE diagnostics on DEMO, taking into account the need to minimize the island size in order to minimize the required control (heating) power to be applied [74]. As an example, the mean detection time for rotating islands in the plasma is shown in Fig. 4 as a function of the mode rotation frequency, with the island size as parameter. An early mode detection within a time of less than 20 ms is possible if the mode is 6 cm wide and rotating with a frequency of at least 30 Hz.

In these simulations, however, beam broadening, deviation and latency effects as induced by plasma turbulence and by actuator properties (accuracy of ECRH steering mirrors etc.) have not been included so far, so that future updates are to be expected.

The second requirement is related to the speed and accuracy which is currently assumed to be achievable by spectroscopy and radiation measurements on DEMO, from which a detailed knowledge of the impurity situation in the plasma can be derived. The given numbers translate practically into an ambitious requirement for the spectroscopic system to be able to identify intensity changes of impurity radiation of one percent with a time delay (integration time and analysis) of not more than 0.2 sec. An early detection of impurity events is desirable to be able to counteract them, e.g. via auxiliary heating (avoiding radiation induced disruptions). Finally, the ELM requirement implies that transient heat loads in the divertor would have to stay below the limit of surface crack formation [75] in the tungsten divertor target, which is a factor ~ 10 lower than the melting threshold of tungsten.

Extensive studies on JET have shown that a fraction of several percent of disruptions remains without clear explanation [76], and that a fraction of several percent of upcoming disruptions is recognized too late for effective mitigation actions [77]. A few more general issues on disruptions are listed below in chapter 6. From the control point of view, it is important to work towards an early and reliable recognition of plasma conditions which may lead to disruptions, to provide means to avoid disruptions, and ultimately to provide means to mitigate a disruption if it cannot be avoided. Typical sensors for imminent disruptions which are used today [78] will be all available on DEMO, but their latency will be somewhat larger as compared to medium sized experimental tokamaks like ASDEX-Upgrade or TCV, because of the mounting position of some diagnostics set well back behind the blanket (see details below). Moreover, the possible reaction time for disruption mitigation will be much longer than on medium sized tokamaks, since

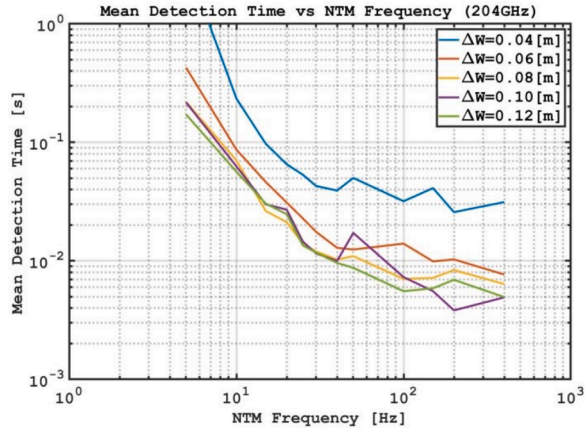

Fig. 4. Mean mode detection time simulated for different mode size and rotation frequencies.

on DEMO the matter injection system (e.g. shattered pellet injector or massive gas injection system) would need to be installed in a location set back behind the blanket in order to ensure sufficient component lifetime and operational reliability within the neutron environment. It will remain an important open issue for the further development of the DEMO physics basis [10,13] to provide a plasma scenario with sufficiently reduced disruptivity, to develop the DEMO device as a whole towards stable operation with almost no disruptions and to achieve a design which provides a certain level of resilience towards some low number of disruptions that cannot be avoided. Also, the control strategy will have to focus on clearly identifying the plasma state and reacting in a proper manner once this state is left, i.e. a strong focus will be on avoidance at an early stage, initiating a shutdown at loss of controllability rather than reacting only when MHD instabilities develop.

As a next step it is planned to develop a supervisory controller for DEMO to handle events, allocating actuators in real-time. This is particularly important in case of exceptions, which are events that require changing the control approach, such as switching to use of a controller that employs a different actuator or changing the control goal. Exception handling requires the definition of the set of exceptions and the development of an automated exception handling approach. One of the problems is managing complexity, since even a concise definition of exceptions will result in a very large number of them. Many requirements for controllers used to execute handling policies are similar to those of nominal control, but there are some important additional constraints: robustness of the new control is paramount, even at the expense of performance. In this framework, model-based predictive control could determine, based on a set of constraints, what the optimum transition is between the initial system state when the exception occurs and a specified stable target system state.

High confinement plasma scenarios with a large gradient of the plasma pressure near the separatrix often exhibit edge localized modes (ELMs), i.e. an instability which periodically expels up to 20 percent of the pedestal energy within a short time scale to the plasma-wetted parts of the first wall. To estimate the situation for DEMO, we assume a typical pedestal energy of $W_{ped} \sim 300$ MJ, an ELM duration of $\tau_{ELM} \sim 0.2$ ms and an ELM energy deposition width at the divertor of ~ 20 cm (i.e. spreading of the energy deposition in the divertor by a factor 4 as compared to the stationary heat distribution [79]). Under these assumptions, the maximum heat impact factor reaches

$$\eta_{ELM} \sim 0.2\, W_{ped} \Big/ \left(A_{eff}\sqrt{\tau_{ELM}}\right) \sim 240 \frac{MJ}{m^2\sqrt{s}},$$

exceeding the limits for surface damage (crack formation) for bulk tungsten [80] by a factor 40-80. ELM mitigation factors of this magnitude within ELMing discharges have not yet been demonstrated experimentally over long periods so far [81]. A caveat is that the numbers above were derived assuming that ELMs always 'burn through' the detached divertor and deposit their full energy; so it is at present not clear what fraction of the energy can be buffered by the detached divertor in DEMO. Clearly, the avoidance or mitigation of ELMs down to tolerable levels represents a significant challenge for plasma control, aiming for reliable operation over a large number of long discharges. It is currently assumed that for DEMO a plasma scenario will become available which is either free from ELMs or which exhibit only small ELMs, such that ELM mitigation techniques can be applied in order to meet the requirements for the maximum transient loads to the divertor and first wall, see e.g. [10]. Candidate actuators for ELM mitigation are the pellet injection and edge perturbations induced by resonant magnetic perturbation coils [81,82].

Within the current WPDC project, the specific developments towards control of all core MHD instabilities are still in an early stage. Clearly, a good spatial coverage by diagnostics with high temporal and spatial resolution will be needed to be able to detect any MHD modes sufficiently early. The ECE diagnostic in a "quasi-inline" configuration with

ECRH localised current drive is foreseen as the primary approach for mode control, however, an initial analysis shows that only rotating modes above a certain rotation speed can be detected early enough with this method. Other diagnostics may contribute to MHD mode detection as well, in particular in-vessel coil based magnetic sensors, microwave reflectometry, radiation power / soft x-ray (SXR) measurements, infrared interferometry/polarimetry, and perhaps the neutron/gamma diagnostics.

Impurity events represent a major issue of concern for DEMO control, since already the addition of a few milligrams of the dominant first wall element tungsten to the core plasma may drive the radiation level above the limit and hence trigger a disruption. Fast detection of changes in the tungsten radiation level in the plasma edge region is foreseen by vacuum ultra-violet (VUV) spectroscopy. The possible counter-measures are the reduction of impurity seeding and the increase of auxiliary heating. First numerical studies have been undertaken [53] and are being further refined to explore the limits.

4. Initial suite of diagnostics for DEMO plasma control and their integration in DEMO

The current suite of diagnostics for plasma control on DEMO has been chosen after reviewing the diagnostics foreseen for ITER, according to several criteria. First of all, diagnostic methods have been selected according to their technical simplicity and robustness, in the sense of low vulnerability (high durability) of the required most forward mounted components in the presence of the adverse effects arising from irradiation, particle fluxes, and thermal and mechanical loads in DEMO. The second goal has been to provide a full coverage of the plasma control issues with sufficient redundancy both in terms of number of methods and diagnostic channels or lines of sight, in order to obtain reliable information on the plasma status under all foreseeable plasma conditions, and even under circumstances where a number of sub-systems or channels would fail. Finally, some more general issues like the compatibility of the required in-vessel diagnostic components to remote handling were taken into account. The list of all diagnostic methods and channels is presented in table 3.

Some details of this suite of diagnostics and their integration approaches will be further elaborated in the following.

4.1. Introduction to diagnostic integration approaches on DEMO

For the in-vessel integration of diagnostics into the DEMO tokamak, several key approaches are foreseen. First, five or six of the 16 equatorial port plugs (EP) located on the horizontal mid-plane of the tokamak are reserved for integration of diagnostics and related components [83]. Second, a limited amount of space is assumed to be available for diagnostic integration in several of the vertical ports (VP) located on the top side of the machine. Within these port plugs (EP and VP), it is foreseen to integrate diagnostic components such as first wall apertures allowing access to the plasma, diagnostic ducts providing penetrations e.g. for light or neutrons to pass through, as well as metallic mirrors and mirror holders, waveguides and cabling. Third, the diagnostic slim cassette approach has been developed as a modular approach for the integration of those diagnostics which require access to the plasma from a wide range of poloidal locations [84], which is the case e.g. for microwave reflectometry and magnetic sensors. Finally, a thermo-current measurement will be implemented in the divertor cassette, where three different options are being evaluated [85,86].

4.2. Magnetic diagnostics

4.2.1. Purpose of measurements

As already discussed in Section 3.1., magnetic diagnostics (coil based and Hall sensors) have a wide range of applications, comprising the measurement of plasma position and shape, the diamagnetic energy,

Table 3
Overview on all diagnostic methods and channels foreseen for plasma control on DEMO (EP: equatorial port plug; VP vertical port plug; DSC diagnostic slim cassette).

Diagnostic method	Measurement role	Number of channels / detectors / lines of sights
Inner vessel tangential and normal pick-up coils	Plasma current and plasma centroid position. Vertical speed. Shape and Equilibrium.	2 × 4 × 30
Outer vessel tangential and normal pick-up coils	Plasma current and plasma centroid position. Vertical speed. Shape and Equilibrium.	2 × 4 × 69
Outer vessel flux loops	Shape + equilibrium. Loop voltage. Eddy currents.	8
Inner vessel flux loops	Shape + equilibrium. Loop voltage. Eddy currents.	6
Inner vessel diamagnetic loops	Plasma magnetic energy.	4
Outer vessel diamagnetic loops	Plasma magnetic energy.	4
Outer vessel Rogowski coils	Plasma current	4
Inner vessel Hall sensors	Plasma current and plasma centroid position. Vertical speed. Shape + equilibrium.	2 × 4 × 30
Outer vessel Hall sensors	Plasma current and plasma centroid position. Vertical speed. Shape + equilibrium.	2 × 4 × 69
Outer vessel Faraday sensors	Plasma current and plasma centroid position. Shape + equilibrium.	to be defined
Neutron camera	Neutron flux measurement, from which fusion power, vertical and radial position can be derived. Neutron spectroscopy from which fuel ion ratio and ion temperature can be derived.	2 x (13 + 12) = 50 (EP + VP)
Gamma detectors	Measurement of the gamma-ray spectra in the 16-20 MeV region (yielding information on fusion power and DT ratio)	5-10 channels if well justified
MW reflectometry	Evaluating the position of the separatrix (or another peripheric density layer) for reconstruction of the shape and position of the plasma.	2 × 5 × 16 (DSC)
Electron cyclotron emission	To measure the electron temperature and associated temperature fluctuations. MHD instability control (magnetic islands) in conjunction with Electron Cyclotron Current Drive (ECCD)	2 × 4 (to be confirmed)
IR polarimetry/ interferometry	Density control (core and edge); MHD detection; vertical position control during start phase.	1 × 9 (EP)
Divertor thermo-current measurements	Power exhaust control, measuring current flowing to divertor target plates, and sheath induced voltage for detachment control	48 div. cassettes, coolant tubes as shunt resistor
Radiation power (core)	Core plasma radiation power, for control of Psep MHD control; suppl. for plasma position control	2 x (13+ 12) = 50 (EP + VP)
X Ray spectroscopy (core)	Line radiation and core plasma concentrations of Kr, Xe and W. Contributes to Ti measurement.	2 × 3 (EP)
VUV spectroscopy (core)	Line radiation and concentrations of all relevant impurities.	2 × 4 (EP)
VUV spectroscopy (edge)	Fast control of the seeded impurity. Line radiation and concentrations of all relevant impurity species (from He to W).	2 × 3 (EP) +2 × 2 × 3 (VP)
		2 x (2 + 3) (EP)

(continued on next page)

Table 3 (*continued*)

IR/VIS/nearUV divertor spectroscopy	Detachment control (position of ionisation front; impurity seeding into divertor); divertor thermography	
VIS spectroscopy and thermography (limiters)	Monitoring of protection limiters	4 (EP)
H_alpha monitoring of pellet injection	Control of pellet success	1 for each of the 2 pellet injection regions (EP)
Collective Thomson Scattering	Fast ion density and velocity distribution	to be defined

plasma current, loop voltage and the detection of MHD modes and instabilities.

4.2.2. Integration of magnetic diagnostics in DEMO

Magnetic pick-up and/or saddle coils will be integrated into the machine at well shielded locations behind the blanket or an equivalent shielding block. In order to achieve good poloidal resolution and provide some capability to detect toroidal variations, 30 poloidal locations at each of 4 toroidal locations are foreseen to be equipped with one radially and one poloidally oriented in-vessel sensor. At the proposed mounting locations the expected time resolution will be somewhat reduced by the eddy current shielding due to the metallic material between plasma and sensors, but still fast enough to be used for plasma position and shape control, as initial simulations using the CREATE equilibrium code [39] show. Such magnetic sensors consist of cabling and metallic housing, as well as ceramic insulators. The adverse effects arising from neutron and gamma irradiation on DEMO will be stronger than on ITER, as previously discussed. Moreover, the spurious voltages arising e. g. from thermoelectric effects (e. g. RITES, TIEMF) from these will be time-integrated over the long discharge duration on DEMO, which may appear as a slowly varying drift of the evaluated signals over time. Hence the applicability and durability of these sensors under DEMO conditions and the long-term stability of measured signals from in vessel inductive sensors needs to be clarified.

Low Temperature Co-fired Ceramic (LTCC) [87] or Thick Printed Copper (TPC) [88] are candidate technologies for the manufacturing of inductive sensors, while the cable connections can be based on the Mineral Insulated Cable (MIC) concept which has been adopted for ITER [89].

For the integration of these magnetic pick-up or saddle coil diagnostics, a modular approach has to be developed, since otherwise the individual treatment of the multitude of components and their attachment points in the machine would make any maintenance work much too time-consuming. For this reason, a crescentic support frame is under consideration, which would carry a number of sensors together with their cabling, and be mounted as one part either to the blanket system or to the inner vessel wall. Depending on the geometry of such support structure, the cables would be routed towards feedthroughs located at vertical or equatorial ports. Integration details such as cable attachments, sensor and cable cooling and the durability against forces during disruptions are still to be defined.

Another large number of magnetic coil based diagnostics will be mounted outside the vacuum vessel, where the irradiation level and resulting spurious voltages are much lower than for in-vessel installation. Due to the strong eddy-current shielding from the vessel, these ex-vessel sensors will have a low time resolution and therefore cannot replace the role of in-vessel sensors for equilibrium control. These ex-vessel measurements would rather be used as a slow but precise backup measurement, which can e.g. be used for calibration purposes of the in-vessel diagnostics (e.g. integrators). The poloidal distance between neighbouring ex-vessel pickup coils is chosen to be similar to the distance of neighbouring in-vessel coils, resulting in 69 poloidal positions per toroidal location. With 4 toroidal positions, and one radially and one poloidally oriented ex-vessel coil per position, the total set comprises 552 pick-up coils, or 276 pick-up coils and 276 saddle coils. In addition, a number of Rogowski coils are foreseen for plasma current measurement [90], diamagnetic loops for measurement of the diamagnetic energy of the plasma, and flux loops for the measurement of the loop voltage.

It should be noted here that on ITER quite a number of additional in-vessel magnetic sensors will be mounted for technical purposes such as the measurement of halo or eddy currents in the blanket or divertor modules, which may be generated by disruptions. Such sensors are not foreseen as part of the plasma D&C concept for normal operation in DEMO, and are hence not treated here. However, if they will be needed on DEMO, they will be subject to strong deterioration from irradiation effects and hence their implementation on DEMO will not be straightforward.

Along with the in-vessel inductive sensors, a similar number of up to 240 in-vessel Hall sensors may be integrated into the vacuum vessel. Technically, the development of an integrated magnetic sensor consisting of one inductive and one Hall sensor (or 2 by 2, with radial and poloidal orientation) is under consideration. Compared to coil-based magnetic measurements, Hall sensors do not need any time integration of signals and hence could provide stable measurements of the magnetic field over long times. However, technical issues with the temperature dependence of the Hall constant and with the low level of Hall signal for sensors based on thin metal films need to be clarified and resolved [91,92,93]. Specifically, the necessary correction of the temperature dependence of the Hall constant will require an accurate measurement of the local temperature of the sensor. Thus, for each Hall sensor a number of six cable wires has to be provided. As with coil based magnetic diagnostics, the long-term applicability of in-vessel Hall sensors will depend on the durability against DEMO relevant loads, which still needs to be demonstrated. In addition, up to 552 ex-vessel Hall sensors are foreseen, which are meant to provide long-term stable signals without suffering from the degradation arising from neutron irradiation. However, the time resolution of the resulting measured signals from ex-vessel Hall sensors is reduced by the eddy current shielding from the thick vacuum vessel. The metallic Hall sensors under discussion here consist of a thin metal film (e.g. bismuth [91], gold [94] or chromium [95]) on a ceramics substrate (Si3N4, AlN or Al2O3), as well as the cabling (copper, with ceramics insulators). An experimental real-time testing of the endurance of Hall sensors based on the high-temperature nanosized metal gold films has been performed directly in the process of their irradiation with reactor neutrons up to DEMO-relevant fluence [94]. The results confirm the reliable stability of signals of gold sensors in a DEMO-relevant radiation environment up to a fluence of 10^{24} n/m^2, and demonstrate that such values are not yet the limit. In addition, bismuth Hall sensors were tested before and after irradiation, and found to be sufficiently durable against neutron radiation levels up to 2.5×10^{22} n/m^2 [91], while this level of the neutron fluence is not the limit. The natural limit for the maximum operational temperature of pure bismuth based Hall sensors is the melting temperature of Bi of 271.4 °C, however this limit was overcome by adding a small fraction of copper or antimony [92]. In an experiment using a Bi70Sb30 mixture, a Hall sensor has been operated up to a temperature of 390 °C without melting.

In accordance with preliminary estimations of neutron fluxes and fluence for 6 full power years at the Hall sensors locations [30], three groups of areas can be distinguished in DEMO depending on the level of expected fluence. These include: Group I with fluence of (10^{20}-10^{22}) n/m^2 - six ex-vessel areas in which magnetic diagnostics can be provided with metal sensors based on bismuth and semiconductor sensors based on thin InAs films; Group II with (10^{24} - 10^{26}) n/m^2 - four in-vessel areas and one ex-vessel area near the divertor, in which sensors based on gold nanofilms can be used; Group III with (10^{25} - 10^{26}) n/m^2 - three areas with maximum fluence, where the sensors based on gold nanofilms and other materials that are currently being studied can be used. R&D in the

area of Hall sensors has been accompanied by intense research on control electronics implementing advanced features including synchronous detection, a current spinning technique, offset cancellation circuitry etc. [96] which are essential to cope with the low signal levels of most metallic Hall sensors to be operated in the noisy environment of DEMO.

For the future, R&D on the development of radiation hard prototype magnetic sensors is foreseen, followed by irradiation testing with an appropriate neutron source for a fluence in the order of up to 10^{25} n/m^2, which is the relevant range for a sensor location on DEMO behind the blanket.

In addition to the magnetic induction and Hall effect, the Faraday effect can be used to measure the magnetic field strength. Faraday sensors determine the rotation angle of the polarization of a laser beam passing through a transparent material with a high Verdet constant. A Faraday diagnostic for the measurement of the plasma current, based on spun fibres installed around the vacuum vessel, is under development for ITER [97]. Quite recently, an initial study has been started to explore the applicability of this method for DEMO, and results will be presented in a future paper.

4.3. Microwave diagnostics (MW reflectometry and ECE)

4.3.1. Purpose of measurements

Microwave reflectometry will be used on DEMO for the measurement of the plasma density in the gradient region (control of pedestal top density with respect to the density limit) as well as for the position of the plasma boundary (gap control). An initial concept assessment was published in [98]. The plasma (electron) temperature profile will be measured via ECE, limited to the plasma region where the electron density is high enough to provide optical thickness. Additionally, both measurements have important capabilities for the fast detection of rotating MHD modes and instabilities in the plasma.

4.3.2. Integration of microwave diagnostics in DEMO

The frontend components for both MW reflectometry and ECE measurements consist of metallic horn antennae and waveguides. The irradiation conditions and thermal loads acting onto these MW components will be similar to those for the blanket first wall (antennae only slightly set back from the first wall level). Thus, if the front part of these MW components would be made from Eurofer (ferritic steel) with tungsten coating for providing reasonable electrical conductivity, which is the material choice for the blanket and first wall, a component lifetime similar to the blanket lifetime could be expected. Other material choices such as copper or alloys with high conductivity would provide somewhat lower microwave attenuation (typically about 0.2 dB/m for standard sized small waveguides) but the durability of such material combinations near the first wall location of DEMO needs to be verified. The MW components will be actively cooled using a cooling concept similar to that of the blanket to keep their temperatures within the operational range for the materials used. With this technical approach, it is expected that the lifetime of MW antennae will be similar to the lifetime of the blanket.

Microwave (MW) reflectometry measurements are foreseen for 16 different locations around a poloidal circumference. This installation will be duplicated in another sector in order to provide redundancy. Near the mid-plane of the plasma, the “single pair” approach for emitting and receiving antennae will provide good spatial resolution. However, near the upper and lower side, the curvature of the plasma (variation of incidence angles) will cause significant problems for the operation and accuracy of reflectometry measurements. Here, each measurement location will require 4-6 antennae to ensure that the reflected beam is captured by at least one of these antennae, even under conditions of unusually large plasma-wall distance, plasma displacement or instabilities. Using spline methods for interpolation between neighbouring reflectometer locations, the overall accuracy of the boundary reconstruction can be somewhat improved and faulty measurements can be identified [99].

The primary integration approach is via the “dummy poloidal section” or diagnostic slim cassette (DSC) concept [84], i.e. two full banana-shaped housings (inboard and outboard) with a toroidal dimension of 20-30 cm, carrying the antennae and waveguides, and routing these waveguides towards the vertical port, see fig. 5.

This dummy poloidal section might be integrated with an entire breeding blanket (BB) sector. Whenever the blanket will be exchanged, the microwave waveguides would be disconnected near the vertical port and the entire BB sector together with the dummy poloidal sector would be replaced using a similar procedure to that of the blanket banana exchange. A new BB sector would then be inserted and the waveguides connected again to the extensions via the vertical port [84]. A first analysis of this concept with regard to nuclear and thermal aspects was presented in [101], and an improved version in [102].

The possibilities and limitations of equilibrium control for DEMO based on microwave reflectometry shall be further analysed by simulation studies and demonstrated by validation experiments (R&D) on current tokamaks such as ASDEX-Upgrade.

For the ECE measurements, which will be used for the measurement of the electron temperature profile and for MHD control, a sufficient spatial resolution can only be obtained when measuring from the outboard mid-plane side of the plasma [74]. At the current stage, two poloidal access locations (one equatorial, one at a poloidal angle close to or coincident with the electron cyclotron current drive (ECCD) system designed for neoclassical tearing mode (NTM) control) are suggested for each toroidal sector at four toroidal locations to preserve the capability of phase detection of n=2 toroidal number modes (8 lines of sight in total). ECE antennas with apertures of less than 100 mm diameter are envisaged, connected with transmission lines of ~60-90 mm inner diameter [103].

4.4. Spectroscopic and radiation measurements

4.4.1. Purpose of measurements

For the burn control in conjunction with power exhaust control, a precise measurement of the radiated power in the main plasma is needed in order to determine the power flux crossing the separatrix, P_{sep}, see Eq.

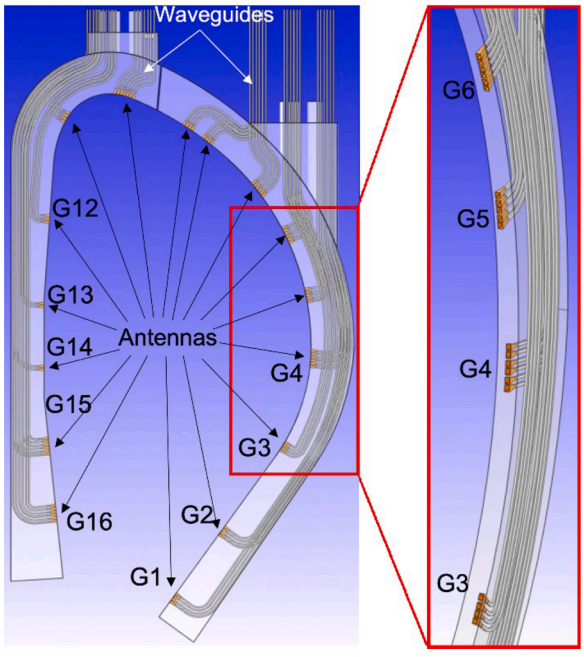

Fig. 5. DSC concept with reflectometer antennae and waveguides integrated therein [100].

(1) in Section 3.2 above. Furthermore, for detachment control the existence of a cold plasma region near the divertor target or an ionization front in the divertor plasma has to be monitored via a detailed spectroscopic analysis of the divertor plasma. This analysis may also yield information on the local tungsten erosion rate in the strike point region of the divertor, which needs to be minimized in order to achieve high availability over long operational periods on DEMO. Direct measurement of the divertor target temperature via thermography is quite desirable as an additional route for heat load control, however, a detected temperature increase would only indicate with some delay that the heat load has already increased, such that the remaining time span for counter-actions by the control system is short. Thus, such temperature increase may only serve as a back-up or as an ultimate triggering event to turn on the strike point sweeping. For any divertor views from the equatorial plane in the current DEMO configuration, it has to be noted that direct lines of sight towards the strike point region may not be achievable if a divertor dome of usual dimensions would be installed or if a "long-leg" (super-x) divertor geometry would be used (due to shadowing). For all divertor views, it remains to be clarified how far one can rely on the toroidal symmetry of divertor radiation, i.e. how many different toroidal locations should be monitored such that any overloading of one of the divertor targets can be reliably excluded.

To facilitate the feedback-control of the influx of gaseous seed impurities (for radiation control), the intensities of their most prominent spectral lines should be measured, preferably from the edge plasma, since here the fastest response of signals can be achieved (due to the finite impurity transport time scales). Central accumulation of high Z impurities can be identified based on intensity ratios between spectral lines radiated from the plasma core and plasma edge, respectively, which requires using X-ray and VUV spectroscopy in order to access relevant ionization stages at the high plasma temperatures on DEMO. Moreover, the success rate of the pellet fuel injection will be monitored quantitatively via H_α measurements. Finally, the foreseen outer midplane limiters on DEMO may need to be monitored with respect to wall loads, erosion and wall temperature. The latter measurement may also serve as additional input to control the plasma shape and position, since any noticeable load during normal operation would indicate an insufficient distance of the plasma from the limiter.

4.4.2. *Integration of spectroscopic and radiation measurements in DEMO*

The most vulnerable front-end components of spectroscopic and radiation diagnostics are the first mirrors, which serve to collect the light from the plasma and reflect it in radial direction, where secondary mirrors may be located, finally guiding the light towards detectors or spectrometers, which will be located outside of the vacuum vessel. Considering the large neutral particle fluence expected on DEMO, the deterioration of mirror surfaces by erosion and deposition of plasma particles can only be minimized by mounting the mirrors behind long thin ducts with a large length-to-diameter L/D, and providing a dilute gas density within the duct to slow down incoming energetic particles via collisions. According to recent modelling results [104], the eroded and/or deposited layer can be kept smaller than about one tenth of the wavelength per full power year, if a duct with ratio of $L/D > 40$ is used in the infrared range, $L/D > 50$ in the visible and $L/D > 80$ in the VUV wavelength range, respectively, with a deuterium gas density in the order of 3×10^{19} m^3 (equivalent to 0.1 Pa at room temperature) at the duct aperture facing the plasma. Additionally, the nuclear heating of the mirrors has to be limited to preserve the integrity of the optical imaging, even when assuming metallic mirrors with active cooling. These erosion and nuclear heating issues practically rule out the use of mirrors mounted in any forward position, and hence any wide-angle viewing or imaging optical schemes, such as those in the JET [105] and ITER wide-angle viewing systems [106] or the ITER core charge exchange recombination spectroscopy (CXRS) diagnostics [107,108], appear not to be feasible under these conditions. Wherever profile information or a wide coverage of large areas within the DEMO plasma are needed, these can only be accomplished by installing a number of individual narrow (large L/D) lines of sight, with all first and secondary mirrors mounted in set back positions. Following these considerations, front-end optical mirrors on DEMO will be typically installed at 1-2 meters distance from the aperture in the first wall, the latter with a diameter in the range of 3-5 cm. For the material choice of these mirrors, in addition to the maximisation of reflectivity in the wavelength range of interest, also the resilience against adverse effects such as surface erosion, corrosion and high ambient temperatures have to be taken into account. The detailed material selection for optical mirrors on DEMO will need further analysis in future, taking advantage e.g. from ITER results, and conducting dedicated R&D for DEMO first mirrors where needed.

For the spectroscopic measurements listed in Table 3 above, a total of 48 individual lines of sight is proposed in order to achieve the required spatial coverage for all foreseeable plasma conditions, and to obtain some level of redundancy to ensure reliable operation. The mirror surface materials have to be defined according to the wavelength range of interest. For the infrared (IR), visible (VIS) and near-ultraviolet (UV) wavelength range, single-crystalline rhodium appears to be a promising option, providing high reflectivity and good resilience against the ingress of hot water steam in case of leakage of a water cooling system [109]. The mirror systems for IR/VIS/UV spectroscopic systems for divertor, limiter and pellet observations are expected to be implemented in equatorial port plugs. Each line of sight typically consists of an aperture of a few cm diameter, followed by a set of 4-6 mirrors arranged to form a labyrinth in an equatorial port plug, thereby guiding the light to an exit window while inhibiting neutron streaming. In the port cell behind the port plug, the light can be separated into different wavelength ranges (IR, VIS, UV) by beam splitters and then relayed to spectrometers and detectors located in more remote locations. The proposed spectroscopic views into the divertor region from an equatorial port plug are shown in Fig. 6. The entire plasma region between outer and inner divertor target can be monitored separated into three viewing systems (violet), while the radiation distribution along both divertor targets can be measured using two more views (in red).

Some more details on the lines of sight, optical concepts, mechanical design and nuclear analysis have been published in [110,111,112].

In order to cover intense spectral lines from all relevant plasma impurities, a set of vacuum ultraviolet (VUV) spectrometers will be used which cover the wavelength range from 4 nm up to 125 nm, divided into 4 different wavelength bands arranged sequentially to provide good spectral resolution over the entire range. In this wavelength interval, mirrors have to be arranged with grazing incidence in order to achieve sufficiently high reflectivity. The design concept for the DEMO VUV spectrometers closely follows the approach used for similar systems developed for the stellarator Wendelstein 7-X [113] and the tokamak

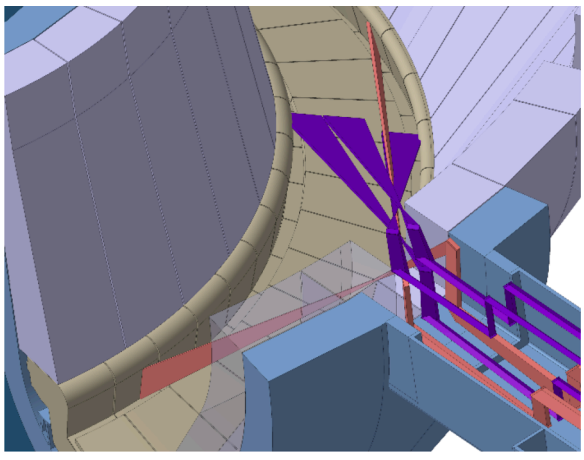

Fig. 6. Spectroscopic lines of sight for the divertor detachment control from an equatorial port plug.

ITER [114].

The design concept for high resolution X-Ray spectroscopy on DEMO also closely follows the developments in progress for ITER [115]. For these spectrometers, a perfect crystal (of quartz or silicon) will serve as the dispersive element, where the distance to the first wall could be at a distance of about 11 meters (duct length), so that radiation induced damage of that crystal should be of minor importance. The use of an additional broadband Bragg reflector mounted at 1-2 meters distance from the first wall is being considered as an option, which would allow deflecting the line of sight in order to keep the direct neutron streaming to the rear of the port at an acceptable level. The Bragg reflector represents itself a relatively large crystal operating at a Bragg angle of 10°-30° and having a general form of a sinusoidal or logarithmic spiral. The major advantage of this complex shape is the following: an arbitrary point source of emission, placed for instance inside the Rowland circle of the Bragg reflector, is imaged as a narrow line on the Rowland circle at the detector. Such approach is currently considered in the next generation of x-ray spectrometers for a laser produced plasma [116]. Such solution requires however a rather accurate matching between the Bragg reflector and the main crystal.

The general approach for the IR/VIS/nearUV spectroscopic systems using pinhole apertures with a first mirror set back radially by a significant distance, while still allowing for some field of view, results in relatively large optical elements and large beam waists within the port plug region. Also the X-Ray spectroscopy requires a sizeable duct dimension, which is getting wider towards the first wall due to the angular dependence from Bragg reflection. This leads to a crowded situation for the optical paths and components in an equatorial port plug, see Fig. 7.

The only subsystem designed without any mirrors or Bragg reflectors is the core radiation power measurement, where 50 straight lines of sight (2 toroidal locations, 13 equatorial and 12 vertical lines of sight each) with detectors placed at locations of lower irradiation levels (behind the vacuum vessel or bioshield) are envisaged. The mounting of the detectors outside the vacuum vessel would facilitate replacement in case of failure. For traditional metal foil based bolometer detectors we can expect at such a location only very low signal intensities due to a very small étendue of the individual lines of sight. Therefore, semiconductor type or gas detectors such as GEM detectors are currently under consideration as alternative to traditional bolometers. For the near future, R&D on comparative detector testing under DEMO relevant conditions is foreseen, in order to demonstrate that detector schemes other than the traditional bolometry are able to achieve sufficiently high accuracy for the control of the total radiated power.

For many of the lines of sight, in particular involving all X-ray, VUV and total radiation measurements, vacuum extensions with high vacuum conditions are needed along the light paths up to the detectors, since the radiation would otherwise be absorbed by e.g. windows or by the gas in the lines. Assuming individual vacuum extensions for all channels of the radiation power measurement (core), while combining some of the VUV and X-ray channels into common vacuum systems, this results in more than 60 vacuum extensions beyond the port plug closure plates, of varying complexity. Window-type interfaces near the port plug plates may be applicable for the visible and infrared lines of sight, if a reasonable technical solution for the windows can be found. In the other case, vacuum extensions may be required for many of the visible and infrared lines of sight as well. Where such vacuum extensions transgress the tritium containment role of the vacuum vessel or cryostat, special safety provisions such as fast high reliability gate valves triggered by the machine safety system will be required.

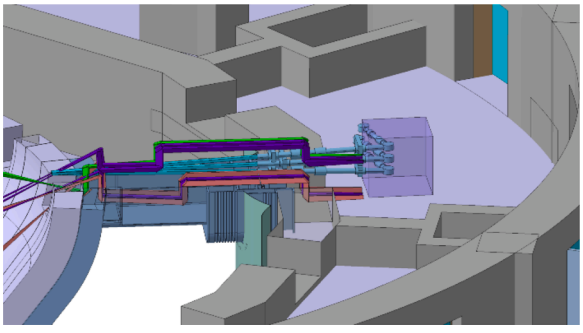

Fig. 7. Port plug integration study comprising X-Ray spectroscopy (light blue), divertor views (red and violet) and pellet monitoring (green).

4.5. Polarimetry/interferometry

4.5.1. Purpose of measurements

Interferometry/Polarimetry can contribute to various aspects of the control scheme. The primary purpose will be to determine a coarse plasma density profile control, including the central density and the pedestal. In addition, the diagnostic can provide core plasma position information to the vertical stability controller during all phases of the discharge, including the break-down and ramp phases.

4.5.2. Integration of polarimetry/interferometry in DEMO

The geometry of the wavelength of the beam path will be similar to the ITER TIP (Toroidal Interferometer/Polarimeter) concept [117]. The alternative ITER PoPola (Poloidal Interferometer/Polarimeter) [118] approach has been ruled out since it would require optical components at the inboard side of the machine where the achievable duct length is too short to ensure long mirror lifetime, and where mirror service via remote maintenance is very difficult. In addition, the strong magnetic fields result in strong cross-coupling effects on the measured Faraday rotation due to the Cotton-Mouton-effect. These can be expected to occur simply because of manufacturing and alignment errors.

Similar to the ITER TIP three mid-plane measurement beams lead from a single port-plug to the ports within sight to the side of the central column. This mid-plane array will be expanded by additional vertical measurement arrays symmetrically placed above and below the mid-plane cords, resulting in a total number of 9 beams. The vertical array will span a distance defined by the maximum port-plug-height (currently around ±1 m above and below the mid-plane). These additional measurement cords will enable vertical stability control with measurement accuracy of the order of a centimetre during the burn-phase and “vertical-plasma-confinement” during the start-up phase. The latter refers to the plasma column being vertically “confined” to the area spanned by the vertical array. A few more physically different lines of sight may become available if retro-reflectors can be mounted in some of the vertical ports. These oblique lines of sight in the equatorial and vertical ports would however occupy a relatively large space (blocking the insertion of radial “drawers” into a major part of the affected port plugs). The implementation of a second set of identical beams on DEMO seems not possible due to space restrictions. The required overall reliability therefore has to be guaranteed via designing each of the nine interferometer beams with independent subsystems of very low failure rate (e.g. independent lasers for each beam).

The wavelength of choice will be a 10 μm/5 μm combination. Higher wavelengths suffer from unacceptable levels of refraction, where the *currently* available laser sources have been considered. Lower wavelengths bear a high risk, as the plasma facing mirrors have been shown to degrade significantly at those wavelengths. The plasma facing mirrors are set back by at least 1 m to 2 m from the plasma with metal tubes for additional protection. Similar to the mirrors for spectroscopy discussed in Section 4.4., the material choice will have to take into account the maximisation of reflectivity in the wavelength range of choice, and the resilience against adverse effects at the foreseen mounting locations. For the secondary mirrors which are set back further and hence will experience lower loads, it is assumed that the requirements are somewhat relaxed and noble metals like Gold may be used to minimize reflection

losses. The window material of choice is zinc-selenide (ZnSe), as diamond has an unfavourable dip in the transmissivity at 5 μm. However, even though ZnSe is a fairly neutron resilient glass, it will have to be placed well away from the neutron irradiated zone to prevent darkening. The possibility of reducing the radiation-induced darkening of windows by continuous or intermittent heating to a few hundred degrees C will be considered.

The system is currently thought to become a dispersion interferometer, due to the improved vibration compensation and resilience to certain phase drifts. It also offers the possibility to build a single pass system with laser and detector in completely different parts of the DEMO assembly, potentially reducing transmission losses and alleviating some of the construction constraints. However, the limited achievable frequency doubling efficiency as well as the high levels of transmission losses are issues to be investigated further. If the beam intensity problems for the dispersion interferometer could not be solved, the alternative option would be two-colour interferometry using two independent lasers.

The combination with polarimetry is an option to recover from a signal loss and can be included in either the two-colour or the dispersion interferometer base. However, the effect of surface erosion and neutron irradiation on the polarization properties of the first mirror need to be investigated. Deposition is known to be a problem for polarization sensitive diagnostics such as Motional-Stark-Effect spectroscopy [119, 120].

Both interferometry and polarimetry will suffer from significant levels of relativistic effects. Ray tracing simulations show that the interferometric phase error is expected to make up between 3 and 6 percent for the TIP geometry during the burn phase, depending on the line of sight. However, independent of the magnitude of the relativistic error, the vertical stability control is not affected by it, due to the geometry chosen for the measurement.

Since it is now accepted that phase drifts due to thermomechanical and electromechanical distortions (and neutron-induced swelling etc.) can be expected to cause significant drifts in the interferometric measurement, phase drift compensation schemes must be employed to keep these to a minimum. For this the safest approach is to settle for a combination of measures: dry-air flooded or evacuated beam ducts should be used where possible to minimize absorption of the 5 μm radiation and minimize phase drifts [121]. In addition real-time monitoring of the local conditions concerning refraction, especially on the source and detector side should be combined with a real-time drift compensation [122]. Both have been shown to work in existing systems.

4.6. Neutron/gamma diagnostics

4.6.1. Purpose of measurements

The DEMO concept for neutron [123] and gamma diagnostics [124] largely follows the ongoing developments for ITER [125]. For the measurement and control of the fusion power, a measurement of the radial profile of the neutronflux will be implemented. During the burn phase, these measurements may also contribute to the plasma position control. The feasibility of a reliable plasma position measurement based on neutron flux measurements has recently been demonstrated on JET [126]. In addition to these, the D/T ratio and ion temperature can be deduced from neutron/gamma spectroscopy.

Gamma spectroscopy of DT 16.63 MeV gamma-ray fusion reaction is also being investigated as an option to obtain an independent measurement of the fusion power at low count rates, allowing for a cross-calibration of the faster neutron flux measurements, and together with the ~20MeV T(p, γ)^{4}He line emission can provide an assessment of the ratio of tritium and deuterium concentrations in the plasma core. Additional R&D may be needed in future to demonstrate and validate the feasibility of gamma spectroscopy for this 16.63 MeV reaction with low cross section under DEMO relevant conditions.

4.6.2. Integration of neutron/gamma measurements in DEMO

The neutron flux measurement system consists of a set of 2 × 13 horizontal lines of sight from an equatorial port and a set of 2 × 12 lines of sight from a vertical port (wider coverage of radial range, and coverage of Shafranov shift effects), where the factor 2 provides some redundancy. The vertical lines of sight are shown in fig. 8.

It remains to be clarified whether the additional gamma-ray spectroscopic measurements can made by using (sharing) the lines of sight of the neutron flux measurement (without significantly compromising their performance), and which level of measurement accuracy could be achieved depending on an assessment of the DT neutron to gamma-ray branching ratio. Currently a certain minimum number of 5-10 lines of sight is considered which may be used to derive a signal for cross-calibration of the faster neutron cameras.

The front-end of each channel consists of a long duct with < 7 cm inner diameter. At the far end of each collimator a detector (or series of detectors) will be mounted (outside the bio-shield) at a distance > 15 m from the front collimator. The low activation steel EUROFER is considered the main material of the collimator tube surrounded by boron carbide B_4C. Material composition of the collimator towards the detector can include material for moderation of in-scattered neutrons (concrete) doped with thermal neutron absorbers and gamma-ray attenuator material.

The lines of sight can be integrated in a poloidal plane, such that the space occupation in the ports is minimized. Specifically, the lines of sight from the equatorial port could be integrated into drawers.

At the location of the detectors (several meters away from the first wall), the irradiation levels are low enough that no adverse effects on the detectors are expected.

Initial assessment of the performance of the neutron flux monitors indicates that the fusion power can be calculated with a relative error of less than a few percent on a time scale of less than 10 ms, and that the neutron emissivity profile can be reconstructed up to the 0.9 normalized poloidal flux coordinate with the same time resolution and a relative error less than 1 percent. From the neutron spectra, the fuel ion ratio and

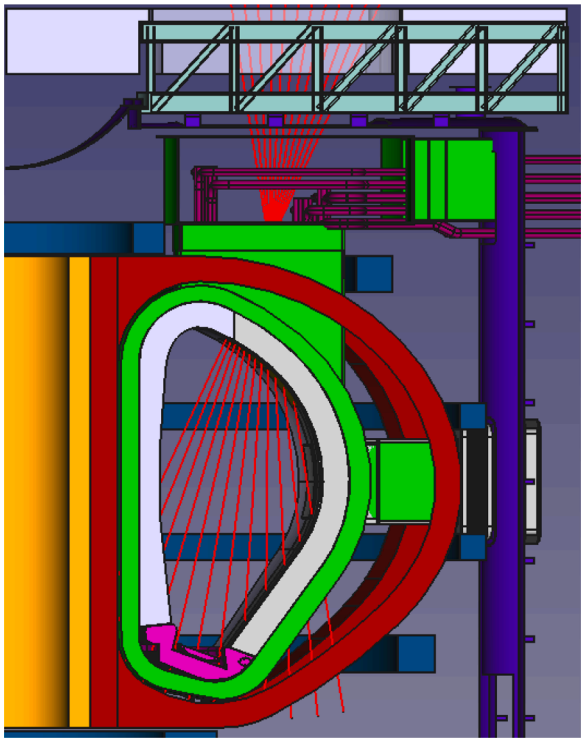

Fig. 8. Poloidal cross section with vertical lines of sight of the neutron diagnostics.

the ion temperature can be determined with a time resolution of 1 second. From these measurements, using the horizontal and vertical neutron lines of sight, the vertical and horizontal (core) plasma position in the burn phase can be determined with a time resolution of 1 ms and with a sensitivity of 8 mm. For the validation of the accuracy of neutron flux measurements for DEMO, R&D is planned on the testing of detectors under DEMO relevant conditions.

4.7. Divertor thermo-current measurement

4.7.1. Purpose of measurements

For power exhaust control, the divertor thermo-current on DEMO shall be measured as the potential difference between the inner and outer divertor target plates or a measurement of the current flowing between the target plates by a Rogowski coil wound around the divertor cassette body. Such a measurement could be used as a reliable indicator of plasma detachment, since under conditions of decreasing plasma temperature in front of the target with increasing puffing rates the sheath voltage and thermo-current tends to zero. The regulation of divertor thermo-currents by impurity puffing feedback control would limit the heat load and erosion of the plasma facing components to an acceptable level and ensure safe steady state operation. This principle of plasma detachment control has been successfully demonstrated on the ASDEX Upgrade tokamak [127]. Thermo-current measurements for each of the 48 DEMO divertor cassettes are planned.

4.7.2. Integration of thermo-current measurements on DEMO

On DEMO, the divertor target plates have to be actively cooled and are electrically connected to the divertor cassette. Nevertheless, there is a finite resistance across the divertor cassette and the thermo-current generates a small voltage that could be measured. Experimental results from ASDEX Upgrade show that using the divertor cassette as a shunt a signal level of 0.75 mV can be measured in the small ELM regime [86].

An alternative approach would employ ceramic insulators to electrically insulate the plasma facing components and water cooling pipes from the divertor cassette. However, the modelling [85] has shown that shunt resistors between the water cooling pipes and the divertor cassette are still needed. These safety shunts protect the water cooling pipes from damage by pipe crushing or boiling water in the stainless steel water cooling pipes after a disruption caused by a vertical displacement event [85]. The final number of safety shunts, their optimal locations and values of resistance are given by the permissible upper limit to the currents generated by a disruption. A preliminary estimate of the signal levels produced by four 600 μΩ safety shunts, connecting the divertor cassette with the water cooling pipes entering the target plates, and considering parallel current paths in the divertor, yields a signal of 64 mV assuming a 150 A thermo-current for a DEMO divertor cassette.

The durability of insulators under the neutron load conditions in the DEMO divertor area (expected neutron fluence up to $10^{25}/m^2$) would still need to be verified. The ambient temperature is in the range of 200-300°C (assuming a water-cooled divertor). However, there are a number of other difficulties to be overcome to make this proposal a viable option. The greatest difficulty with this proposal is the research, development and radiation testing required to realise electrical isolation of the water cooling pipes connecting the plasma facing components and the divertor cassette.

A preliminary estimate of the signal levels produced by a Rogowski coil around the DEMO divertor cassette assumes a sensitivity of 24.5 kA/V as planned for the ITER divertor cassette Rogowski coil [86]. It has been recognised that the vacuum vessel attachment of the divertor cassette provides an alternative path for the thermo-current. Preliminary calculations suggest that 33% of the current would flow through the divertor cassette and 66% would flow through the vacuum vessel wall. A Rogowski coil wound around the cassette with approximately 50 A thermo-current therefore would only have an expected a signal level of 2 mV [86]. Open questions regarding the ability to produce accurate long time scale measurements with electronic integration of the Rogowski coil output and a robust design to survive expected neutron fluxes and temperature ranges will need further detailed studies. Experimental evidence from ASDEX Upgrade shows that the quality of the compensation of pickup signals produced by the poloidal field coils and the plasma current needs to be improved before this measurement can be used as an input signal for feedback control of the heat load to the plasma facing components [86]. Further R&D is under planning to explore and validate the limits of measuring low and noisy thermocurrent signals under DEMO relevant conditions.

5. Actuator properties relevant to plasma control

The essential actuators available for plasma control are the magnet system (poloidal field coils and central solenoid), the auxiliary heating system, and the matter injection (fuel and impurities) and pumping system. The main properties are briefly and qualitatively summarized below. More detailed actuator specifications are under elaboration as part of the development of a consistent overall DEMO concept during the next project phase until 2027.

Six poloidal field (PF) coils will be installed on DEMO to control the equilibrium (plasma shape and position), which also depends on the plasma pressure and current density profiles. The central solenoid (CS) coil serves to provide most of the flux needed to drive the plasma current over the projected burn time of 2 hours. The CS coil consists of several sectors which can be controlled independently, arranged in a “pancake” like arrangement. The total available flux will be in the range of several hundred volt-seconds, while the maximum rate of change will be designed such that a toroidal electric field of 0.3 V/m can be sustained for a period of a few seconds in order to facilitate the ignition of the discharge. The typical maximum voltage of 10 kV to be applied to the coil feeders is defining a limit for the ramp-up and ramp-down speed of the PF and CS coil fields. In order to facilitate a fast control of the vertical and horizontal core plasma position, the installation of in-vessel control coils in addition to the ex-vessel PF coils is being considered. More details can be found in an accompanying paper [128].

The auxiliary heating system to be installed on DEMO is currently not yet fully defined [61]. The main control tasks are as follows:

- Heating during the plasma initiation and current ramp-up, including overcoming the H mode threshold
- Burn control, impurity control and instability control during all plasma phases
- Plasma handling in case of unforeseen events, such as impurity events or component failures.
- Wall conditioning, if applicable.

It is generally assumed that the auxiliary heating system will consist first of the electron cyclotron resonance heating (ECRH) subsystem, comprising in the order of 50 gyrotrons, launchers and corresponding transmission lines, furthermore it may include a neutral beam injection (NBI) subsystem consisting of 2-3 NBI boxes, and finally it may include other subsystems such as ion cyclotron resonance heating (ICRH) and/or lower hybrid (LH) heating. The working assumption during the phase 2014-2020 has been to have ECRH, NBI and ICRH each with 50 MW available, which sums to a maximum auxiliary power of 150 MW to be injected into the plasma. For the next phase of the project (2021-2027), a starting assumption of having only ECR heating with a total power in the range of $P_{ECRH} \sim 130 \ldots 150$ MW has been adopted [61]. The final suite of heating systems will depend on future technical developments as well as on the details of the plasma control requirements, which in turn depend on the details of the DEMO plasma scenario, all of which are not fully defined yet.

Finally, pellet injection is foreseen as the primary approach for DT fuel injection, since for pellets a deeper radial deposition can be

achieved compared to gas injection [59]. In addition however, some DT gas injection is planned for the control of the separatrix plasma density which is related to the divertor detachment. Injection of xenon is foreseen as the main approach for the control of the core plasma radiation power, while argon injection could be used to enhance divertor radiation and facilitate achieving detachment. The long reaction time between the opening of a gas valve outside the bio-shield, and the arrival of injected gas in the plasma, as well as the short radial penetration length of thermal (gaseous) impurity particles into the plasma, may require installing additional means of fast impurity injection such as laser blow-off or high-Z pellet injection. This has to be explored quantitatively by future R&D and simulations.

6. Avoidance of disruptions

One of the most critical issues for the operation and control of the DEMO plasma is the avoidance and mitigation of disruptions. Extrapolating the results from investigations related to JET [129] and ITER [130], in a disruption on DEMO up to 50% of the thermal plasma energy of ~ 1.3 GJ would be released to the first wall within the predicted short thermal quench period of ~ 1-2 ms duration. If this energy is distributed over the entire first wall area (~2000 m^2) with an inhomogeneity factor of 3-4, which is usually referred to as the case of perfect disruption mitigation, the resulting heat impact factor reaches $\eta = W_{th}/A_{eff}/\sqrt{\tau_{TQ}} \sim 30\ MJ/m^2\sqrt{s}$, which is about half of the value needed for the melting of bulk tungsten starting from the DEMO operational temperature (~ 300-500°C), but significantly exceeding the limit for surface crack formation. It remains the subject of future R&D to determine how many of such events the first wall and divertor of DEMO could withstand. Obviously, since well mitigated disruptions on DEMO may lead to large-area wall damage, disruption avoidance should have highest priority on DEMO.

The main root causes for disruptions are briefly listed, explaining the envisaged counter-measures from the point of view of DEMO control:

1) The vertical plasma position in a divertor tokamak is in principle unstable, since the plasma current centroid is subject to attractive forces from the poloidal field coils located above and below the plasma, which grow inversely to the distance to the respective coils. If a deviation of the vertical plasma position from the nominal position is recognized too late, the counter-action by the poloidal field coils may come too late and the plasma would touch the wall and eventually disrupt. The risk for this type of disruption can be minimized by limiting the plasma elongation and shaping, which unfortunately reduces the nominal fusion power according to the confinement scaling law, moreover by introducing a conducting shell within the tokamak for passive stabilisation via eddy-currents, and finally by optimizing the control system with respect to performance (accuracy and speed) and reliability of all relevant measurements and actuators. This specifically means that PF coils should allow for performing sufficiently fast control actions in case of plasma movement. Here, the installation of in-vessel control coils would provide significant advantages with regard to higher control speed (less eddy current shielding) and lower power demands (lower volume enclosed as compared to ex-vessel coils). The feasibility of implementing in-vessel control coils of suitable long life under DEMO conditions is still to be demonstrated.
2) Various types of MHD instabilities may be generated in particular when operating the plasma near the operational limits, causing loss of confinement quality and eventually disruptions. Clearly, these paths to disruptions can be counteracted by providing means for early and reliable recognition of any instabilities evolving, and choosing the plasma scenario with sufficient distance from operational limits. Here, the diagnostic coverage relevant for MHD mode control still needs to be verified.
3) Failures of the control system (component or system failure) may also lead to disruptions. Here, a systematic improvement of the reliability of any part of the control system is needed, and a certain amount of redundancy with respect to both the number of systems/channels and the number of methods has to be installed, depending on the practically achievable level of reliability of the respective systems. Here, the currently assumed redundancy factor of 2 for all diagnostics still needs to be validated as part of the overall analysis of reliability, availability, maintainability and inspectability (RAMI). Plasma operation with reduced redundancy on individual diagnostic systems after failure of a few diagnostic systems is assumed permissible.
4) The number of disruptions arising from human error in the operation of DEMO and its control system should in principle be reduced over time by the fact that DEMO will finally and ideally be operated within one stable discharge scenario only, while the control system will be steadily matured along with increasing operational experience, defining rigorously the allowed operational domain. However, before this point can be reached, many components will need to pass rigorous testing and validation procedures, and many operational issues will have to be demonstrated experimentally on ITER first. After this, the commissioning phase of DEMO will have to include a step-by-step approach, where the operational parameters will be only gradually adjusted towards the final ones. A quantitative development of a commissioning strategy for DEMO is still pending.
5) Unforeseen events, e.g. large impurity influxes, wall damage with coolant ingress or the quench of a superconducting magnet are a matter of concern: above a certain size or speed of the event, the disruption cannot be avoided at all and the control system could only (if at all) reduce but not avoid machine damage. Therefore, the minimization of the risk of such unforeseen events should have high priority in the DEMO design. This in particular means design optimisation aiming for robust and reliable components, low wall loads and small amounts of eroded and deposited wall material.

For all the possible disruption causes listed above, the reduction of their probability will involve quite expensive design choices. It should also be noted that the operation of DEMO during the commissioning phase may be susceptible to a higher disruptivity, since the necessary fine-tuning procedure towards the final stable plasma regime with good performance will include final experimental verification at operational conditions which are realized for the first time on DEMO, and hence will naturally be associated with a higher failure rate. Elaborating the details of a safe commissioning programme on DEMO will be the subject of future work.

7. Summary and conclusions

The development of the D&C system for a future tokamak demonstration fusion reactor (DEMO) is a challenging task, which comprises a variety of physics and technology elements and interfaces with many areas of the overall DEMO design. The requirements for reliable and stable plasma control in DEMO are much higher than in any existing fusion device, since DEMO should achieve an overall availability that goes far beyond what experimental tokamaks have achieved so far, while operational failures resulting in plasma disruptions should be strictly avoided because of the risk of severe damage to the inner DEMO components. For the task of controlling the DEMO plasma scenario, the detailed parameters of which are not yet fully defined, only a limited set of diagnostics and actuators will be available. Within the Pre-Concept Design Phase for DEMO, an initial allocation of diagnostics and actuators to the main control tasks has been developed, and some of the main approaches for their integration as well as their expected performance have been explored. Novel integrated control techniques may help to improve the reliability of DEMO plasma control and overcome the limitations arising from diagnostics and actuators, in particular by

providing an accurate forecast on the evolution of the plasma state based on sophisticated modelling.

Obtaining a quantitative understanding of DEMO control is a prerequisite for achieving the required control reliability. For this purpose, the performance of control components and the overall control system are being analysed by quantitative simulations and, where needed, validation experiments on the feasibility of specific approaches towards DEMO plasma control have to be performed.

For many plasma parameters the DEMO operational point will have to obey control margins (distance from operational limits), the required size of which will depend on the actual accuracy that the control system will be able to achieve. In this regard, the feasibility of the DEMO control system will have a strong impact on the overall DEMO design, since larger control margins lead to a reduction of fusion power which could only be compensated by e.g. enlarging the dimensions of the tokamak. Thus an iterative approach is needed, where the DEMO physics and technology basis, the design details and the development of the D&C system are pursued in parallel.

CRediT authorship contribution statement

W. Biel: Project administration, Investigation, Writing – review & editing. **M. Ariola:** Project administration, Investigation, Writing – review & editing. **I. Bolshakova:** Investigation. **K.J. Brunner:** Investigation. **M. Cecconello:** Investigation. **I. Duran:** Investigation. **Th. Franke:** Project administration, Investigation. **L. Giacomelli:** Investigation. **L. Giannone:** Investigation. **F. Janky:** Investigation. **A. Krimmer:** Investigation. **R. Luis:** Investigation. **A. Malaquias:** Investigation. **G. Marchiori:** Investigation. **O. Marchuk:** Investigation. **D. Mazon:** Investigation. **A. Pironti:** Investigation. **A. Quercia:** Investigation. **N. Rispoli:** Investigation. **S. El Shawish:** Investigation. **M. Siccinio:** Investigation. **A. Silva:** Investigation. **C. Sozzi:** Investigation. **G. Tartaglione:** Investigation. **T. Todd:** Supervision. **W. Treutterer:** Investigation. **H. Zohm:** Investigation.

Declaration of Competing Interest

The authors declare that they have no known competing financial interests or personal relationships that could have appeared to influence the work reported in this paper.

Acknowledgments

This work has been carried out within the framework of the EUROfusion Consortium and has received funding from the Euratom research and training programme 2014-2018 and 2019-2020 under grant agreement No 633053. The views and opinions expressed herein do not necessarily reflect those of the European Commission.

References

[1] A. J. H. Donne et al. (2018) Fusion Electricity - A roadmap to the realisation of fusion energy. [Online]. https://www.euro-fusion.org/fileadmin/user_upload/EUROfusion/Documents/2018_Research_roadmap_long_version_01.pdf.
[2] G. Federici, et al., Overview of the design approach and prioritization of R&D activities towards an EU DEMO, Fusion Engin. Des. 109–111 (2016) 1464–1474, https://doi.org/10.1016/j.fusengdes.2015.11.050 [Online]https://doi.org/.
[3] G. Federici, et al., DEMO design activity in Europe: progress and updates, Fusion Engin. Des. 136 (2018) 729–741, https://doi.org/10.1016/j.fusengdes.2018.04.001 [Online]https://doi.org/.
[4] G. Federici et al., "The EU DEMO staged approach in the Pre-Concept Design Phase," *Fusion Engin. Des., this issue.*
[5] C. Bachmann, et al., Overview over DEMO design integration challenges and their impact on component design concepts, Fus. Engin. Des. 87 (2018) 136, https://doi.org/10.1016/j.fusengdes.2017.12.040 [Online]https://doi.org/.
[6] C. Bachmann, et al., Containment structures and port configurations, Fusion Engin. Des. (2022) *this issue*.
[7] C. Gliss, et al., Integrated design of tokamak building concepts including ex-vessel maintenance, Fusion Engin. Des. (2022) *this issue*.
[8] O. Crofts, et al., EU DEMO remote maintenance system development during the pre-concept design phase, Fusion Engin. Des. (2022) *this issue*.
[9] L.V. Boccaccini, et al., Status of maturation of critical technologies and systems design: breeding blanket, Fusion. Engin. Des. (2022) *this issue*.
[10] M. Siccinio, et al., DEMO physics challenges beyond ITER, Fusion Engin. Des. 156 (2020), 111603, https://doi.org/10.1016/j.fusengdes.2020.111603 [Online] https://doi.org/.
[11] M. Siccinio, et al., Impact of the plasma operation on the technical requirements in EU-DEMO, Fusion Engin. Des. (2022) *this issue*.
[12] E.J. Doyle, et al., Chapter 2: Plasma confinement and transport, Nucl. Fusion. 47 (2007) S18–S127, https://doi.org/10.1088/0029-5515/47/6/S02 [Online] https://doi.org/.
[13] R. Wenninger, et al., The physics and technology basis entering European system code studies for DEMO, Nucl. Fusion. 57 (2017), 016011, https://doi.org/10.1088/0029-5515/57/1/016011 [Online]https://doi.org/.
[14] G. Federici, et al., The plan forward for EU DEMO, Fusion Engin. Des. (2022) *(this issue)*.
[15] A. Costley, et al., Key issues in ITER diagnostics: Problems and solutions, Rev Sci. Instrum. 70 (1999) 391–396, https://doi.org/10.1063/1.1149506 [Online] https://doi.org/.
[16] A.J.H. Donne, et al., Chapter 7: diagnostics, Nucl. Fusion. 47 (2007) S337–S384, https://doi.org/10.1088/0029-5515/47/6/S07 [Online]https://dx.doi.org/.
[17] C.I. Walker, et al., ITER diagnostics: integration and engineering aspects, Rev. Sci. Instrum. 75 (2004) 4243–4246, https://doi.org/10.1063/1.1787609 [Online] https://doi.org/.
[18] A. Costley, et al., Technological challenges of ITER diagnostics, Fusion Engin. Des. 74 (2005) 109–119, https://doi.org/10.1016/j.fusengdes.2005.08.026 [Online]https://doi.org/.
[19] M. Walsh, et al., ITER diagnostic challenges, in: IEEE 24th Symp. on Fusion Engineering, 2011, pp. 1–8, https://doi.org/10.1109/SOFE.2011.6052210 [Online]https://doi.org/.
[20] G. Vayakis, et al., Generic diagnostic issues for a burning plasma experiment, Fus. Sci. Technol. 53 (2008) 699–750, https://doi.org/10.13182/FST08-A1684 [Online]https://doi.org/.
[21] F. Orsitto, et al., Diagnostics and control for the steady state and pulsed tokamak DEMO, Nucl. Fusion. 56 (2016), 026009, https://doi.org/10.1088/0029-5515/56/2/026009 [Online]https://doi.org/.
[22] W. Biel, et al., DEMO diagnostics and burn control, Fusion Engin. Des. 96–97 (2015) 8–15, https://doi.org/10.1016/j.fusengdes.2015.01.046 [Online]https://doi.org/.
[23] W. Biel, et al., Diagnostics for plasma control – from ITER to DEMO, Fus. Engin. Des. 146 (2019) 465–472, https://doi.org/10.1016/j.fusengdes.2018.12.092 [Online]https://doi.org/.
[24] M.L. Walker, et al., Introduction to Tokamak plasma control, in: American Control Conference (ACC), 2020, pp. 2901–2918, https://doi.org/10.23919/ACC45564.2020.9147561 [Online]https://doi.org/.
[25] K. Young, An assessment of the penetrations in the first wall required for plasma measurements for control of an advanced Tokamak plasma demo, Fus. Sci. Technol. 57 (2010) 298, https://doi.org/10.13182/FST10-A9473 [Online] https://doi.org/.
[26] G. Federici, et al., An overview of the EU breeding blanket design strategy as an integral part, Fusion Engin. Des. 141 (2019) 30–42, https://doi.org/10.1016/j.fusengdes.2019.01.141 [Online]https://doi.org/.
[27] J.A. Wesson, et al., Nucl. Fusion. 29 (1989) 641.
[28] M. Siccinio, et al., Impact of an integrated core/SOL description on the R and BT optimization of tokamak fusion reactors, Nucl. Fusion. 58 (2018), 016032, https://doi.org/10.1088/1741-4326/aa9583 [Online]https://doi.org/.
[29] L. Zabeo, et al., Overview of magnetic control in ITER, Fusion Engin. Des. 89 (2014) 553–557, https://doi.org/10.1016/j.fusengdes.2014.03.051 [Online] https://doi.org/.
[30] U. Fischer, et al., Neutronic performance issues of the breeding blanket options for theEuropean DEMO fusion power plant, Fusion Eng. Des. 109-111 (2016) 1458–1463, https://doi.org/10.1016/j.fusengdes.2015.11.051 [Online]https://doi.org/.
[31] S. Peruzzo, et al., Progress in the design and testing of in-vessel magnetic pickup coils for ITER, IEEE Trans. Plasma Sci. 44 (2016) 1704, https://doi.org/10.1109/TPS.2016.2580380 [Online]https://doi.org/.
[32] S. Peruzzo, et al., R&D on ITER in-vessel magnetic sensors, Fusion Engin. Des. 88 (2013) 1302–1305, https://doi.org/10.1016/j.fusengdes.2013.02.018 [Online] https://doi.org/.
[33] E.J. Doyle, et al., Design basis for the ITER plasma shape and position control reflectometer system, in: G. Gorini, P. Prandoni, E. Sindoni, P.E. Stott (Eds.), in Diagnostics for Experimental Thermonuclear Fusion, Springer, Boston, MA, 1998, https://doi.org/10.1007/978-1-4615-5353-3_11 vol. 2[Online]https://doi.org/.
[34] J. Santos, et al., Reflectometry-based plasma position feedback control demonstration at ASDEX Upgrade, Nucl. Fusion. 52 (2012), 032003, https://doi.org/10.1088/0029-5515/52/3/032003 [Online]https://doi.org/.
[35] M. Ariola, A. Pironti, Magnetic Control of Tokamak Plasmas, 2nd Ed., Springer, 2016.
[36] M. Ariola, et al., Simulation of magnetic control of the plasma shape on the DEMO tokamak, Fusion Engin. Des. 146 (2019) 728–731, https://doi.org/10.1016/j.fusengdes.2019.01.065 [Online]https://doi.org/.
[37] T. Hender, et al., Chapter 3: MHD stability, operational limits and disruptions, Nucl. Fusion. 47 (2007) S128, https://doi.org/10.1088/0029-5515/47/6/S03 [Online]https://dx.doi.org/.

[38] L. Giannone, et al., Real-time diamagnetic flux measurements on ASDEX Upgrade, Rev. Sci. Instrum. 87 (2016), 053509, https://doi.org/10.1063/1.4950858 [Online]https://doi.org/.

[39] R. Albanese, F. Villone, The linearized CREATE-L plasma response model for the control of current, position and shape in tokamaks, Nucl. Fusion. 38 (1998) 723, https://doi.org/10.1088/0029-5515/38/5/307 [Online]https://doi.org/.

[40] V.D. Shafranov, *Rev. Prog. Phys.*, M. A. Leontovich, Ed. New York: Consultants Bureau, 1966, vol. 2, pp. 103-151.

[41] E. Schuster, et al., Burn control in fusion reactors via nonlinear stabilization techniques, Fusion Sci. technol. 43 (2003) 18, https://doi.org/10.13182/FST03-A246 [Online]https://doi.org/.

[42] M.D. Boyer, et al., Nonlinear burn condition control in tokamaks using isotopic fuel tailoring, Nucl. Fusion. 55 (2015), 083021, https://doi.org/10.1088/0029-5515/55/8/083021 [Online]https://doi.org/.

[43] V. Graber, et al., Nonlinear burn control in ITER using adaptive allocation of actuators with uncertain dynamics, Nucl. Fusion (accepted) (2021), https://doi.org/10.1088/1741-4326/ac3cd8 [Online]https://doi.org/.

[44] F. Albajar, et al., Improved calculation of synchrotron radiation losses in realistic tokamak plasmas, Nucl. Fusion. 41 (2001) 665, https://doi.org/10.1088/0029-5515/41/6/301 [Online]https://doi.org/.

[45] M. Greenwald, et al., Density profile peaking in low collisionality H-modes: comparison of Alcator C-Mod data to ASDEX Upgrade/JET scalings, Nucl. Fusion. 47 (2007) L26, https://doi.org/10.1088/0029-5515/47/9/L03 [Online]https://dx.doi.org/.

[46] H. Zohm, et al., On the physics guidelines for a tokamak DEMO, Nucl. Fusion. 53 (2013), 073019, https://doi.org/10.1088/0029-5515/53/7/073019 [Online]https://doi.org/.

[47] A. Huber, et al., The effect of the isotope on the H-mode density limit, Nucl. Fusion. 57 (2017), 086007, https://doi.org/10.1088/1741-4326/aa663a [Online]https://doi.org/.

[48] M. Siccinio, et al., A 0D stationary model for the evaluation of the degree of detachment on the divertor plates, Plasma Phys. Control. Fusion 58 (2016), 125011, https://doi.org/10.1088/0741-3335/58/12/125011 [Online]https://doi.org/.

[49] M. Greenwald, A new look to tokamak density limits, Nucl. Fusion. 28 (1988) 2199, https://doi.org/10.1088/0029-5515/28/12/009 [Online]https://doi.org/.

[50] T. Eich, et al., Correlation of the tokamak H-mode density limit with ballooning stability at the separatrix, Nucl. Fusion. 58 (2018), 034001 [Online], https://iopscience.iop.org/article/10.1088/1741-4326/aaa340.

[51] Y.R. Martin, et al., Power requirement for accessing the H-mode in ITER, J. Phys. Conf. Ser. 123 (2008), 012033, https://doi.org/10.1088/1742-6596/123/1/012033 [Online]https://doi.org/.

[52] Th. Eich, et al., Correlation of the tokamak H-mode density limit with ballooning stability at the separatrix, Nucl. Fusion. 58 (2018), 034001, https://doi.org/10.1088/1741-4326/aaa340 [Online]https://doi.org/.

[53] F. Janky, et al., Simulation of burn control for DEMO using ASTRA coupled with Simulink, Fusion Engin. Des. 123 (2017) 555–558, https://doi.org/10.1016/j.fusengdes.2017.04.043 [Online]https://doi.org/.

[54] R. Ambrosino, et al., Sweeping control performance on DEMO device, Fusion Eng. Des. 171 (2021), 112640, https://doi.org/10.1016/j.fusengdes.2021.112640 press[Online]https://doi.org/.

[55] F. Maviglia, et al., Impact of plasma-wall interaction and exhaust on the EU-DEMO design, Nuclear Materials and Energy 26 (2021), 100897, https://doi.org/10.1016/j.nme.2020.100897 [Online]https://doi.org/.

[56] P. Vicenzi, et al., Fuelling and density control for DEMO, Nucl. Fusion. 55 (2015), 113028, https://doi.org/10.1088/0029-5515/55/11/113028 [Online]https://doi.org/.

[57] F. da Silva, et al., Modelling reflectometry diagnostics: finite-difference time-domain simulation of reflectometry in fusion plasmas, J. Instrum. 14 (2019) C08003, https://doi.org/10.1088/1748-0221/14/08/C08003 [Online]https://doi.org/.

[58] P.T. Lang, et al., Optimizing the EU-DEMO pellet fuelling scheme, Fusion Engin. Des. 159 (2020), 111591, https://doi.org/10.1016/j.fusengdes.2020.111591 [Online]https://doi.org/.

[59] Ch. Day et al., "Tritium Fuelling and Vacuum Systems," *Fusion Engin. Des., this issue*.

[60] S.B. Korsholm, et al., Design and development of the ITER CTS diagnostic, EPJ Web Conf. 203 (2019) 03002, https://doi.org/10.1051/epjconf/201920303002 [Online]https://doi.org/.

[61] M.Q. Tran, et al., Status and future development of heating and current drive for the EU DEMO, Fusion Engin. Des. (2022) *this issue*.

[62] M. Siccinio, et al., Figure of merit for divertor protection in the preliminary design of the EU-DEMO reactor, Nucl. Fusion. 59 (2019), 106026, https://doi.org/10.1088/1741-4326/ab3153 [Online]https://doi.org/.

[63] B.L. Welch, et al., Density measurements in the edge, divertor and X-point regions of Alcator C-Mod from Balmer series emission, Phys. Plasmas 2 (11) (1995) 4246, https://doi.org/10.1063/1.871049 [Online]https://doi.org/.

[64] A.G. Meigs, et al., Deuterium Balmer/Stark spectroscopy and impurity profiles: first results from mirror-link divertor spectroscopy system on the JET ITER-like wall, J. Nucl. Mat. 438 (2013) S607–S611, https://doi.org/10.1016/j.jnucmat.2013.01.127 [Online]https://doi.org/.

[65] A. Perek, et al., MANTIS: A real-time quantitative multispectral imaging system for fusion plasmas, Rev. Sci. Instrum. 90 (2019), 123514, https://doi.org/10.1063/1.5115569 [Online]https://doi.org/.

[66] T. Ravensbergen, et al., Development of a real-time algorithm for detection of the divertor detachment radiation front using multi-spectral imaging, Nucl. Fusion 60 (2020), 066017, https://doi.org/10.1088/1741-4326/ab8183 [Online]https://doi.org/.

[67] A. Kallenbach, et al., Electric currents in the scrape-off layer in ASDEX-Upgrade, J. Nucl. Mat. 290-293 (2001) 639–643, https://doi.org/10.1016/S0022-3115(00)00445-1 [Online]https://doi.org/.

[68] T.W. Petrie, et al., Infrared thermography system on DIII-D, Rev. Sci. Instrum. 61 (1990) 3557, https://doi.org/10.1063/1.1141570 [Online]https://doi.org/.

[69] G.V. Pereverzev, P.N. Yushmanov, ASTRA Automated System for TRansport Analysis in a tokamak. Max-Planck-Institut for Plasma Physics, Garching, IPP report 5/98, 2002 [Online], https://pure.mpg.de/rest/items/item_2138238/component/file_2138237/content.

[70] D. Humphreys, et al., Novel aspects of plasma control in ITER, Phys. Plasmas 22 (2015), 021806, https://doi.org/10.1063/1.4907901 [Online]https://doi.org/.

[71] F. Felici, et al., Real-time-capable prediction of temperature and density profiles in a tokamak using RAPTOR and a first-principle-based transport model, Nucl. Fusion. 58 (2018), 096006, https://doi.org/10.1088/1741-4326/aac8f0 [Online]https://doi.org/.

[72] F. Janky, et al., Validation of the Fenix ASDEX upgrade flight simulator, Fusion Engin. Des. 163 (2021), 112126, https://doi.org/10.1016/j.fusengdes.2020.112126 [Online]https://doi.org/.

[73] F. Janky, et al., DEMO control challenges, in: 31st Symposium on Fusion Technology (SOFT), 25 Sept 2020, p. 20, virtual edition.

[74] N. Rispoli, et al., Detection of neoclassical tearing modes in demo using the electron cyclotron emission, Fusion Engin. Des. 123 (2017) 628–631, https://doi.org/10.1016/j.fusengdes.2017.02.067 [Online]https://doi.org/.

[75] M. Wirtz, et al., Thermal shock tests to qualify different tungsten grades as plasma facing material, Phys. Scr. T167 (2016), 014015, https://doi.org/10.1088/0031-8949/T167/1/014015 [Online]https://doi.org/.

[76] P. de Vries, et al., Survey of disruption causes at JET, Nucl. Fusion. 51 (2011), 053018, https://doi.org/10.1088/0029-5515/51/5/053018 [Online]https://dx.doi.org/.

[77] J. Vega, et al., Results of the JET real-time disruption predictor in the ITER-like wall campaigns, Fusion Engin. Des. 88 (2013) 1228, https://doi.org/10.1016/j.fusengdes.2013.03.003 [Online]https://doi.org/.

[78] M. Maraschek, et al., Path-oriented early reaction to approaching disruptions in ASDEX Upgrade and TCV in view of the future needs for ITER and DEMO, Plasma Phys. Contr. Fusion 60 (2018), 014047, https://doi.org/10.1088/1361-6587/aa8d05 [Online]https://doi.org/.

[79] R.A. Pitts, et al., A full tungsten divertor for ITER: Physics issues and design status, J. Nucl. Mat. 438 (2013) S48–S56, https://doi.org/10.1016/j.jnucmat.2013.01.008 [Online]https://doi.org/.

[80] Th. Loewenhoff, et al., Tungsten and CFC degradation under combined high cycle transient and steady state heat loads, Fusion Engin. Des. 87 (2012) 1201–1205, https://doi.org/10.1016/j.fusengdes.2012.02.106 [Online]https://doi.org/.

[81] P.T. Lang, et al., ELM control strategies and tools: status and potential for ITER, Nucl. Fusion. 53 (2013), 043004, https://doi.org/10.1088/0029-5515/53/4/043004 [Online]https://doi.org/.

[82] T.E Evans, et al., ELM mitigation techniques, J. Nucl. Mat. 438 (2013) S11–S18, https://doi.org/10.1016/j.jnucmat.2013.01.283 [Online]https://doi.org/.

[83] Th. Franke, et al., Initial port integration concept for EC and NB systems in EU DEMO tokamak, Fusion Engin. Des. 146 (2019) 1642–1646, https://doi.org/10.1016/j.fusengdes.2019.03.007 [Online]https://doi.org/.

[84] A. Malaquias, et al., Integration concept of the reflectometry diagnostic, IEEE Transact. Plasma Sci. 46 (2018) 451, https://doi.org/10.1109/TPS.2017.2784785 [Online]https://doi.org/.

[85] S. El Shawish, et al., Shunt analysis in the isolated-target divertor model for plasma detachment, Fusion Engin. Des. 161 (2020), 112058, https://doi.org/10.1016/j.fusengdes.2020.112058 [Online]https://doi.org/.

[86] L. Giannone, et al., Shunt and Rogowski coil measurements on ASDEX Upgrade in support of DEMO detachment control, Fusion Engin. Des. 166 (2021), 112276, https://doi.org/10.1016/j.fusengdes.2021.112276 [Online]https://doi.org/.

[87] Y. Imanaka, Multilayered Low Temperature Cofired Ceramics (LTCC) Technology, Springer, New York, 2005.

[88] J. Reboun, et al., Printed thick copper films for power applications, in: 7th Electronic System-Integration Technology Conference (ESTC), Dresden, Germany, 2018.

[89] G. Vayakis, et al., Development of the ITER magnetic diagnostic set and specification, Rev. Sci. Instrum. 83 (2012) 10D712, https://doi.org/10.1063/1.4732077 [Online]https://doi.org/.

[90] A. Quercia, et al., Performance analysis of Rogowski coils and the measurement of the total toroidal current in the ITER machine, Nucl. Fusion. 57 (2017), 126049, https://doi.org/10.1088/1741-4326/aa86fd [Online]https://doi.org/.

[91] I. Duran, et al., Development of Bismuth Hall sensors for ITER steady state magnetic diagnostics, Fusion Engin. Des. 123 (2017) 690–694, https://doi.org/10.1016/j.fusengdes.2017.05.142 [Online]https://doi.org/.

[92] I. Duran, et al., Status of steady-state magnetic diagnostic for ITER and outlook for possible materials of Hall sensors for DEMO, Fusion Engin. Des. 146 (2019) 2397, https://doi.org/10.1016/j.fusengdes.2019.03.201 [Online]https://doi.org/.

[93] S. Entler, et al., Temperature dependence of the Hall coefficient of sensitive layer materials considered for DEMO Hall sensors, Fusion Engin. Des. 153 (2020), 111454, https://doi.org/10.1016/j.fusengdes.2020.111454 [Online]https://doi.org/.

[94] I. Bolshakova, et al., Metal Hall sensors for the new generation fusion reactors of DEMO scale, Nucl. Fusion. 57 (2017), 116042, https://doi.org/10.1088/1741-4326/aa7867 [Online]https://doi.org/.

[95] S. Entler, et al., Ceramic-Chromium Hall Sensors for Environments with High Temperatures and Neutron Radiation, Sensors 21 (2021) 721, https://doi.org/10.3390/s21030721 [Online]https://doi.org/.
[96] S. Entler, et al., Prospects for the steady-state magnetic diagnostic based on antimony Hall sensors for future fusion power reactors, Fusion Engin. Des. 146 (2019) 526, https://doi.org/10.1016/j.fusengdes.2019.01.013 [Online]https://doi.org/.
[97] A. Gusarov, et al., Status and future developments of R&D on fiber optics current sensor for ITER, Fusion Engin. Des. 136A (2018) 477–480, https://doi.org/10.1016/j.fusengdes.2018.03.001 [Online]https://doi.org/.
[98] A. Silva, et al., First assessment of microwave diagnostics for DEMO, Fusion Engin. Des. 96–97 (2015) 948–951, https://doi.org/10.1016/j.fusengdes.2015.06.137 [Online]https://doi.org/.
[99] G. Marchiori, et al., Study of a plasma boundary reconstruction method based on reflectometric measurements for control purposes, IEEE Trans. Plasma Sci. 46 (2018) 1285, https://doi.org/10.1109/TPS.2018.2797549 [Online]https://doi.org/.
[100] J.H. Belo, et al., Design and integration studies of a diagnostics slim cassette concept for DEMO, Nucl. Fusion (submitted) (2021).
[101] R. Luis, et al., Nuclear and thermal analysis of a reflectometry diagnostics concept for DEMO, IEEE Trans. Plasma Sci. 46 (2018) 1247, https://doi.org/10.1109/TPS.2017.2780922 [Online]https://doi.org/.
[102] Y. Nietiadi, et al., Nuclear and thermal analysis of a multi-reflectometer system for DEMO, Fusion Engin. Des. 167 (2021), 112349, https://doi.org/10.1016/j.fusengdes.2021.112349 [Online]https://doi.org/.
[103] J.L. Doane, et al., Design of circular corrugated waveguides to transmit millimeter waves at ITER, Fusion Sci. Technol. 53 (2008) 159–173, https://doi.org/10.13182/FST08-A1662 [Online]https://doi.org/.
[104] M. Tokar, Assessment for erosion of and impurity deposition on first mirrors in a fusion reactor, Nucl. Fusion. 58 (2018), 096007, https://doi.org/10.1088/1741-4326/aac95c [Online]https://doi.org/.
[105] A. Huber, et al., Development of a mirror-based endoscope for divertor spectroscopy on JET with the new ITER-like wall (invited), Rev. Sci. Instrum. 83 (2012) 10D511, https://doi.org/10.1063/1.4731759 [Online]https://doi.org/.
[106] S. Salasca, et al., The ITER Equatorial Visible/Infra-Red Wide Angle Viewing System: Status of Design and R&D, Fusion Engin. Des. 96-97 (2015) 932–937, https://doi.org/10.1016/j.fusengdes.2015.02.062 [Online]https://doi.org/.
[107] W. Biel, et al., Overview on R&D and design activities for the ITER core charge exchange spectroscopy diagnostic system, Fusion Engin. Des. 86 (2011) 548–551, https://doi.org/10.1016/j.fusengdes.2011.02.086 [Online]https://doi.org/.
[108] Ph. Mertens, The core-plasma CXRS diagnostic for ITER: an introduction to the current design, J. Fusion Energy 38 (2019) 264–282, https://doi.org/10.1007/s10894-018-0202-1 [Online]https://doi.org/.
[109] A. Pereira, et al., Steam-resistant optical materials for use in diagnostic mirrors for ITER, IEEE Transact. Plasma Sci. 48 (2020) 1619, https://doi.org/10.1109/TPS.2020.2967460 [Online]https://doi.org/.
[110] W. Gonzalez, et al., Conceptual studies on spectroscopy and radiation diagnostic systems for plasma control on DEMO, Fusion Engin. Des. 146 (2019) 2297–2301, https://doi.org/10.1016/j.fusengdes.2019.03.176 [Online]https://doi.org/.
[111] W. Gonzalez, et al., Preliminary study of a visible, high spatial resolution spectrometer for DEMO divertor survey, J. Instrum. 15 (2020) C01008, https://doi.org/10.1088/1748-0221/15/01/C01008 [Online]https://doi.org/.
[112] R. Luis, et al., Nuclear analysis of the DEMO divertor survey visible high-resolution spectrometer, Fusion Engin. Des. 169 (2021), 112460, https://doi.org/10.1016/j.fusengdes.2021.112460 [Online]https://doi.org/.
[113] W. Biel, et al., Design of a high–efficiency extreme ultraviolet overview spectrometer system for plasma impurity studies on the stellarator experiment Wendelstein 7-X, Rev. Sci. Instrum. 75 (2004) 3268, https://doi.org/10.1063/1.1784557 [Online]https://doi.org/.
[114] C.R. Seon, et al., Design of ITER divertor VUV spectrometer and prototype test at KSTAR tokamak, Eur. Phys. J. D 71 (2017) 313, https://doi.org/10.1140/epjd/e2017-70825-3 [Online]https://doi.org/.
[115] R. Barnsley, et al., Design study for international thermonuclear experimental reactor high resolution x-ray spectroscopy array, Rev. Sci. Instrum. 75 (2004) 3743, https://doi.org/10.1063/1.1790044 [Online]https://doi.org/.
[116] M. Bitter, et al., A new class of focusing crystal shapes for Bragg spectroscopy of small, point-like, x-ray sources in laser produced plasmas, Rev. Sci Instrum. 92 (2021), 043531, https://doi.org/10.1063/5.0043599 [Online]https://doi.org/.
[117] M.A. Van Zeeland, et al., Conceptual design of the tangentially viewing combined interferometer-polarimeter for ITER density measurements, Rev. Sci. Instrum. 84 (2013), 043501, https://doi.org/10.1063/1.4798602 [Online]https://doi.org/.
[118] A.J.H. Donné, et al., Poloidal polarimeter for current density measurements in ITER, Rev. Sci. Instrum. 75 (2004) 4694, https://doi.org/10.1063/1.1804372 [Online]https://doi.org/.
[119] A. Malaquias, et al., Polarization and reflectivity changes on mirror based viewing systems during long pulse operation, in: 30th EPS Conference on Contr. Fusion and Plasma Phys 27A, St. Petersburg, 2003, 7-11 July 2003O-3.4C.
[120] V.S. Voitsenya, et al., Simulation of environment effects on retroreflectors in ITER, Rev. Sci. Instrum. (2005), 083502, https://doi.org/10.1063/1.2001627, 2005[Online]https://doi.org/.
[121] M A Van Zeeland, et al., Plasma Phys. Control. Fusion 59 (2017), 125005, https://doi.org/10.1088/1748-0221/14/11/P11016 [Online]https://doi.org/.
[122] K.J. Brunner, et al., J. Instrum. 14 (2019) 11016, https://doi.org/10.1088/1748-0221/14/11/P11016 [Online]https://doi.org/.
[123] M. Cecconello, et al., Pre-conceptual study of the European DEMO neutron diagnostics, J. Instrum. 14 (2019) C09001, https://doi.org/10.1088/1748-0221/14/09/C09001 [Online]https://doi.org/.
[124] L. Giacomelli, et al., Conceptual studies of gamma ray diagnostics for DEMO control, Fusion Engin. Des. 136B (2018) 1494–1498, https://doi.org/10.1016/j.fusengdes.2018.05.041 [Online]https://doi.org/.
[125] M. Bertalot, et al., Present status of ITER neutron diagnostics development, J. Fusion Energy 38 (2019) 283–290, https://doi.org/10.1007/s10894-019-00220-w [Online]https://doi.org/.
[126] A. Sperduti, et al., Plasma position measurement with collimated neutron flux monitor diagnostics on JET, Fusion Engin. Des. 168 (2021), 112597, https://doi.org/10.1016/j.fusengdes.2021.112597 [Online]https://doi.org/.
[127] A. Kallenbach, et al., Divertor power load feedback with nitrogen seeding in ASDEX upgrade, Plasma Phys. Control. Fusion 52 (2010), 055002, https://doi.org/10.1088/0741-3335/52/5/055002 [Online]https://dx.doi.org/.
[128] V. Corato, et al., The DEMO magnet system - status and future challenges, Fusion Engin. Design (2022) *this issue.*.
[129] M. Lehnen, et al., Impact and mitigation of disruptions with the ITER-like wall in JET, Nucl. Fusion. 53 (2013), 093007, https://doi.org/10.1088/0029-5515/53/9/093007 [Online]https://doi.org/.
[130] M. Lehnen, et al., Disruptions in ITER and strategies for their control and mitigation, J. Nucl. Mater. 463 (2015) 39–48, https://doi.org/10.1016/j.jnucmat.2014.10.075 [Online]https://doi.org/.